An Aerodynamic Study of Bulk Commodity Tractor Trailers

Western Trailer
251 W Gowen Rd., Boise, ID 83716

&

University of Idaho
875 Perimeter Drive, Moscow, ID 83843

Brandon Hilliard
Jake Frost
Liam Johnson

Table of Contents

Abstract

Bulk commodity tractor trailers provide necessary transportation over long distances for various materials, such as cement, asphalt, and wood chips. Heavy-duty semi-trucks tow these large trailers for hundreds of miles, producing a significant amount of air pollution from the truck exhaust. To reduce and classify these emission levels, an aerodynamic study was done on two different Western Trailer bulk commodity tractor trailers – a 48-foot and 53-foot trailer, and a double-trailer setup with a lead and pup trailer, commonly referred to as an A-Train set up. These trailer configurations were constructed with a 1:38.33 modeling scale and placed in an open-circuit wind tunnel at the University of Idaho. Typical trailer modifications were tested on both trailer configurations. Aerodynamic effects, emission outputs, and fuel consumptions were analyzed and quantified for each trailer with each possible modification, including front-end and undercarriage attachments as well as different A-Train lengths.

Introduction

Semi-trucks are used all over the world for transporting goods. They provide easy and affordable methods to keep economies running. The downside is that semi-trucks produce a lot of carbon-dioxide pollution from their exhaust. If the trailers they tow are improved aerodynamically, that carbon-dioxide production can be minimized. Western Trailers Company, headquartered in Boise, Idaho, has a multitude of tractor trailers that have different aerodynamic characteristics. The Trailer Park Boys are tasked with testing and simulating these trailers in various configurations so improvements can be made to meet new tractor trailer requirements that will be implemented in 2018.

Phase 2 of the Heavy-duty Greenhouse Gas and Fuel Efficiency regulations were implemented by the Environmental Protection Agency (EPA) and the National Highway Traffic Safety Administration (NHTSA) to reduce pollution from nationwide trucking. [5] The regulations focus on the grams of Carbon-Dioxide emitted by the truck per ton-mile as well as the fuel consumption rates per 1,000 ton-miles. One ton-mile is equivalent to one ton of freight carried one mile.

Table 1 gives the maximum CO_2 emissions output for trucks with future model years of different trailers. A trailer is classified as short if it is no longer than 50 feet. [5] Otherwise, it is classified as a long trailer. A refrigerated trailer, or van, indicates a fully-enclosed trailer with refrigeration capabilities. All other trailers are considered dry.

Table 1. Maximum limits of CO_2 emissions for different trailer model years (in grams of CO_2/ton-mile).

Model Year	Dry Van		Refrigerated Van	
	Short	Long	Short	Long
2018-2020	125.4	81.3	129.1	83.0
2021-2023	123.7	78.9	127.5	80.6
2024-2026	120.9	77.2	124.7	78.9
2027+	118.8	75.7	122.7	77.4

Table 2 shows the maximum fuel consumption rates for different model years of trailers. Identical classifications in Table 1 are present in Table 2, but the EPA and NHTSA did implement voluntary standards for trailer model years in the near future.

Although Tables 1 and 2 include regulations for refrigerated trailers, Western Trailer only needed documentation for emissions and fuel consumption rates for dry, bulk commodity trailers, which usually carry material such as dirt, wood chips, or asphalt. These models are commonly referred to as a 48-foot trailer and an A-Train trailer (see Figures 1 and 2). Therefore, we only focused on the dry trailer regulations within Tables 1 and 2.

Table 2. Maximum limits for fuel consumption rates for different trailer model years (in gallons of diesel/1,000 ton-miles).

Model years	Dry van		Refrigerated van	
	Long	Short	Long	Short
Voluntary Standards				
2018 to 2020	7.98625	12.31827	8.15324	12.68173
Mandatory Standards				
2021 to 2023	7.75049	12.15128	7.91749	12.52456
2024 to 2026	7.58350	11.87623	7.75049	12.24951
2027 and later	7.43615	11.72888	7.60314	12.10216

Trailer Configurations

Western Trailer is a top 25 trailer manufacturer in North America and produces over 1,000 trailers annually. For this project, only a few bulk commodity tractor trailers needed to be aerodynamically analyzed for the EPA-NHTSA regulations. Figure 1 is a Western Trailer with a recessed bed, commonly referred to as a possum belly. Figure 2 shows a tandem set-up of two Western Trailers, which is called an A-Train set-up. It contains a lead and pup trailer, both with hopper bins attached to the underside.

Figure 1. 53-foot Western Trailer model with a recessed bed (possum belly).

Figure 2. A-Train Western Trailer model with hopper bins. Two bins on the lead trailer, one bin on the pup trailer.

The possum belly trailer is much like other trailer models that are 48 feet long and can have hopper bins attached to the underside as well as a nose cone and bull nose attached to the front end. Along with these various configurations, the trailers can also be without any attachments. Figure 3 is a drawing from Western Trailer that shows a basic 48-foot trailer. Figure 4 is a drawing of a 48-foot trailer with a nose cone and hopper bins.

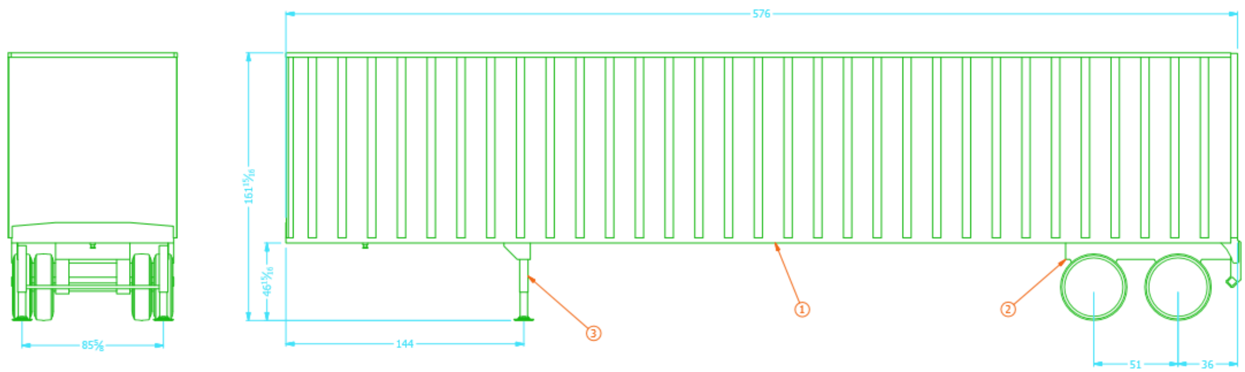

Figure 3. Front and side views of a base-model 48-foot Western Trailer.

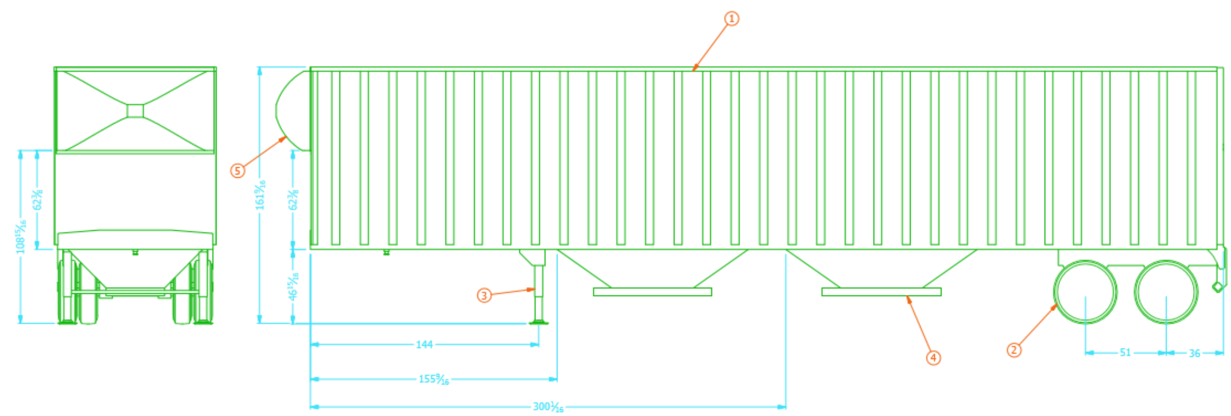

Figure 4. Front and side views of a 48-foot Western Trailer with a nose cone and hopper bins.

The A-Train trailers always have hopper bins attached to the undersides of the lead and pup trailer, but the front ends of each can have a nose cone attached, similar to the one seen in Figure 4. Tongue lengths between the trailers can also vary from seven feet to 21 feet. Figure 5 shows the different tongue lengths Western Trailer offers for their clients.

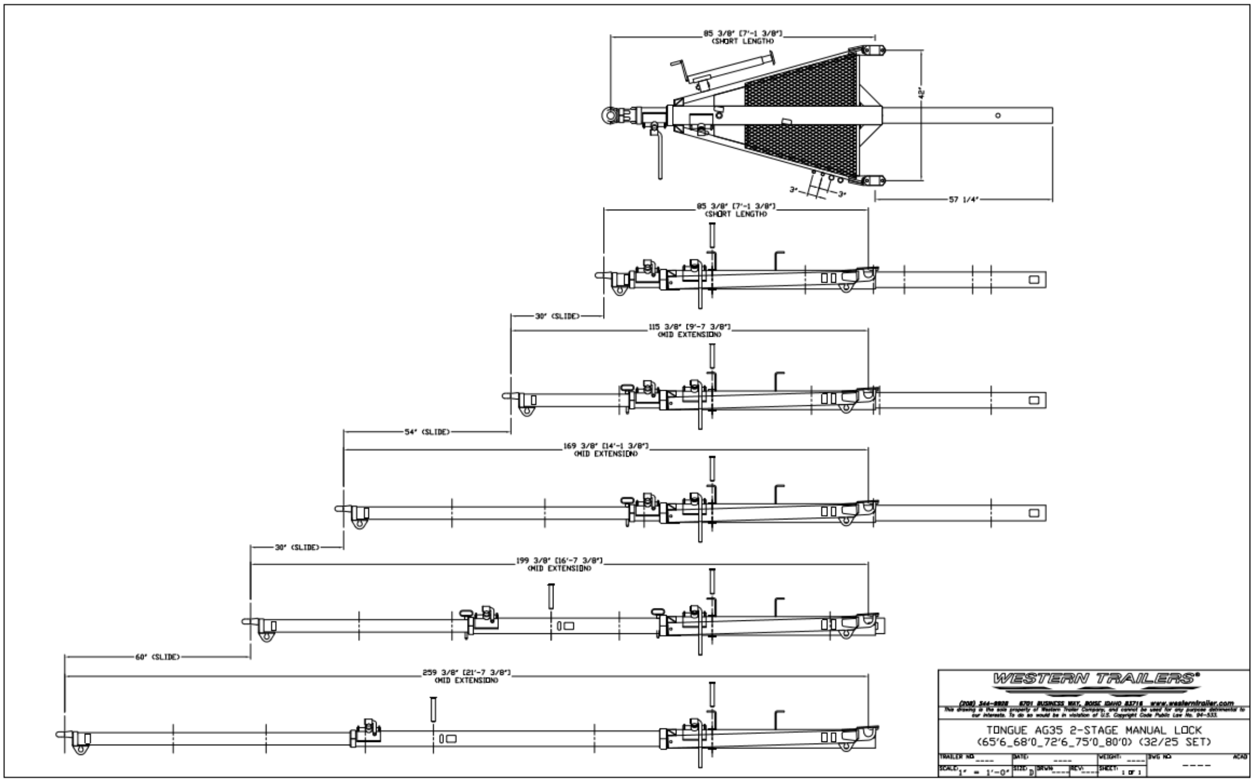

Figure 5. The different tongue lengths Western Trailer offers for their A-Train models.

Modeling Process

At the start of the project, our team was tasked with creating scaled-down models of various Western Trailer products so that we could use the wind tunnel located at the University of Idaho. We decided to base our entire scaling system off our model height being exactly 3 inches. This resulted in a scaling factor of 1:38.33 and an overall blockage ratio of 2.47% - the maximum suggested blockage ratio is 10% with an 18-inch by 18-inch test section. [3] The length and width of the 48-foot trailer models was 15.018 inches and 2.671 inches, respectively. A 53-foot trailer model was the same width, but 16.591 inches in length. The A-Train models also followed this scaling factor, resulting in a height of 2.039 inches and a width of 2.560 inches. The lead trailer is 10.106 inches long and the pup trailer is 7.915 inches long.

Five panels were cut out of 1/8-inch balsa wood (Figure 6) on the laser cutter at the University of Idaho. The five panels included the front, two sides, top, and bottom. An intuitive tooth design was used to ensure correct alignment of all the panels on each model. Wood glue was placed on the edge of each tooth when the panels were assembled.

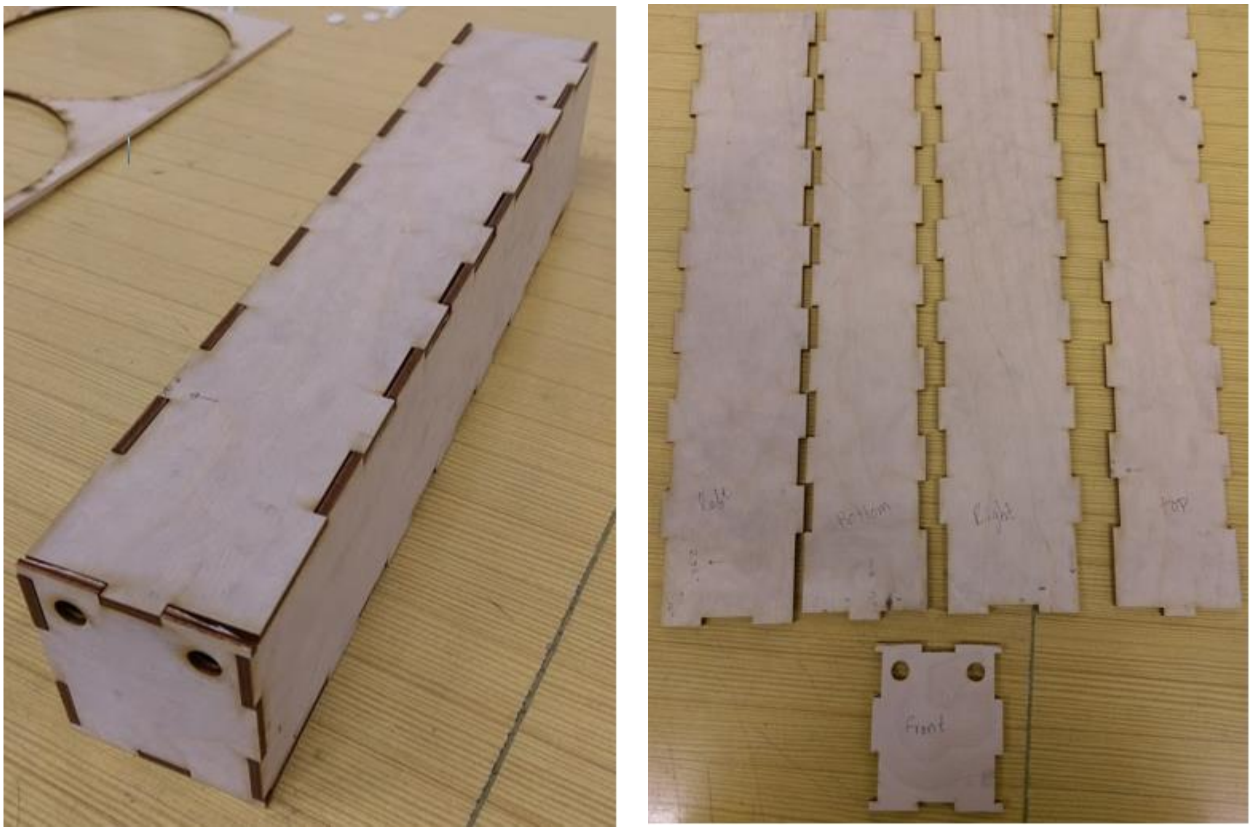

Figure 6. The 48-foot trailer model before and after assembly of the five panels.

Trailer features, such as a nose cone or hopper bin, were 3D-printed with PLA plastic on a 3D Sindoh printer. These features needed to be attached to our trailers for testing, so we decided to use magnets. With each trailer feature, a recessed region would be created in the 3D part for a magnet (Figure 7).

Figure 7. The nose cone attachments were printed with guide cylinders and a center recess to place a magnet.

Inside the trailer, magnets were glued on to the wooden panels in precise locations to ensure correct placement of all features. The exact location was first measured in the SolidWorks model and then marked on the trailer panels before they were completely assembled (Figure 8).

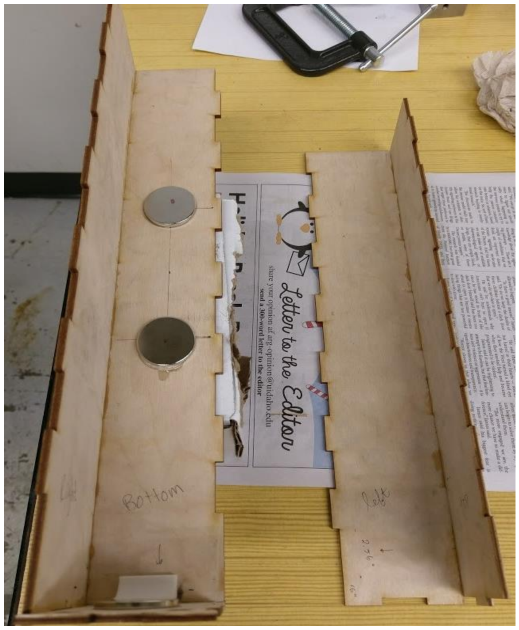

Figure 8. 48-foot trailer partially assembled with magnets.

Figures 9 and 10 give a table-like layout of all the models that were created for testing, along with the five different A-Train trailer lengths in Table 3. The trailer with a possum belly is 53 feet long, unlike the other 48-foot models.

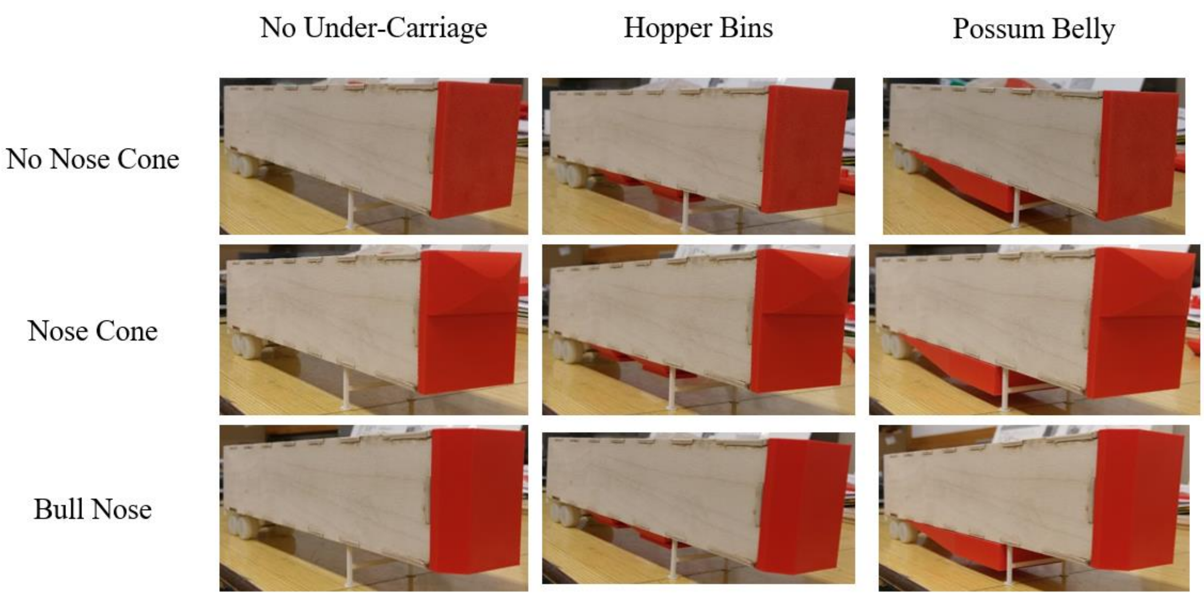

Figure 9. 48-foot and 53-foot trailer configurations, with different front-end and under-carriage attachments.

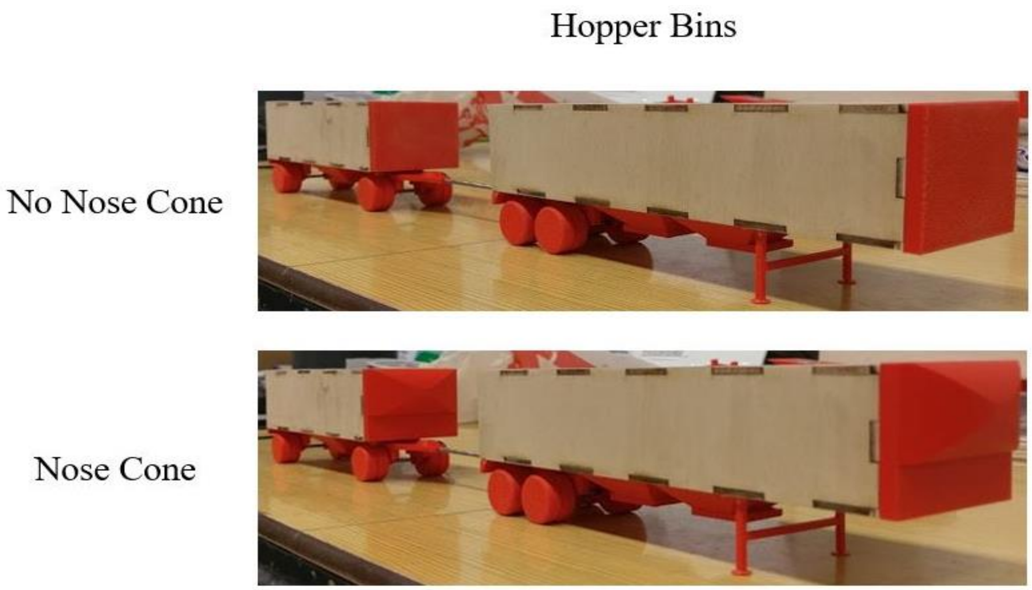

Figure 10. A-Train configurations, with and without a nose cone front-end attachment.

The A-Train trailers always have hopper bins for the under-carriage configuration, so the only variables in testing these models were the front end configurations (with and without a nose cone) and the lengths between the lead and pup trailer (Table 3).

Table 3. A-Train trailer tongue lengths for both the full-size and model trailers.

Full-size Tongue Length	Model Tongue Length
7-foot 1-inch	4.47 inches
9-foot 7-inch	5.26 inches
14-foot 1-inch	6.67 inches
16-foot 7-inch	7.45 inches
21-foot 7-inch	9.02 inches

Wind Tunnel Description

We used the wind tunnel at the University of Idaho, which belongs to the Mechanical Engineering Department. It was implemented in 2000 to facilitate and support hand-on learning for all engineering students. The first project that took advantage of the full functionality of the wind tunnel was in 2001 for a senior-level mechanical engineering class testing parachutes. [7]

The wind tunnel is an open circuit that has a 50-hp, variable frequency drive motor to power a 48-inch axial fan that pulls the air through the 18-inch x 18-inch x 36-inch test section, which is made from ¾-inch plexiglass with removable top and bottom panels. No more than a 10% blockage ratio is recommended for testing. The maximum wind speed the fan can achieve is 160 mph. [3]

As seen in Figure 11, the wind tunnel has an Eiffel shape with the test section closer to the entrance. A smooth transition from square to round occurs when traveling through the test section to prevent any turbulence that could distort any data acquisitions.

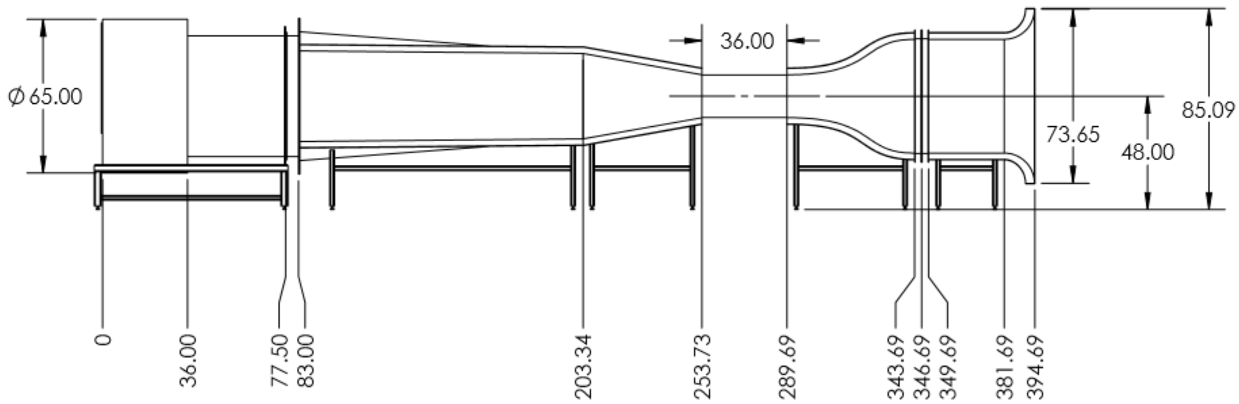

Figure 11. A side view of the wind tunnel with basic dimensions.

Aside from the test section, the entire wind tunnel is made from fiberglass. There is a metal honeycomb mesh just past the entrance of the wind tunnel to straighten the inlet flow before it encounters the test section.

Testing Procedures

Testing began with turning on the visual displays for the wind tunnel. This was important because the electronics of the wind tunnel take approximately 15 minutes to warm up before accurate data can be recorded. These displays show lift force and drag force (N), wind velocity (m/s), pitching moment (N-m), and angle of attack (degrees) (Figure 12).

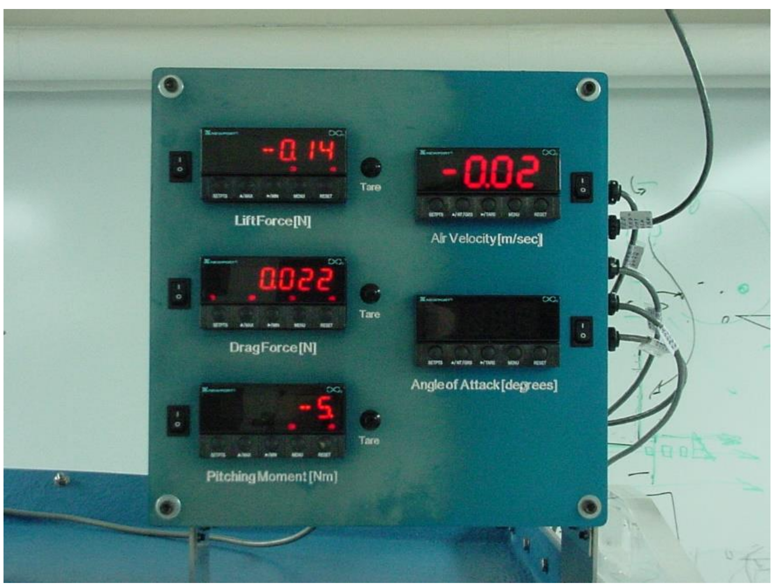

Figure 32. Electronic displays used to acquire data.

Next, we mounted and leveled our trailers onto the wind tunnel sting to ensure the proper and safe orientation within the testing section. Once the trailers were correctly setup, we tested our models with an air velocity ranging from about 30 mph to roughly 78 mph. We determined this range of speeds from preliminary testing (Figure 13), which showed that the drag coefficient follows a linear trend at higher speeds, more specifically at about 30 mph and up. Appendix B contains a more detailed process for setting up the wind tunnel experiments.

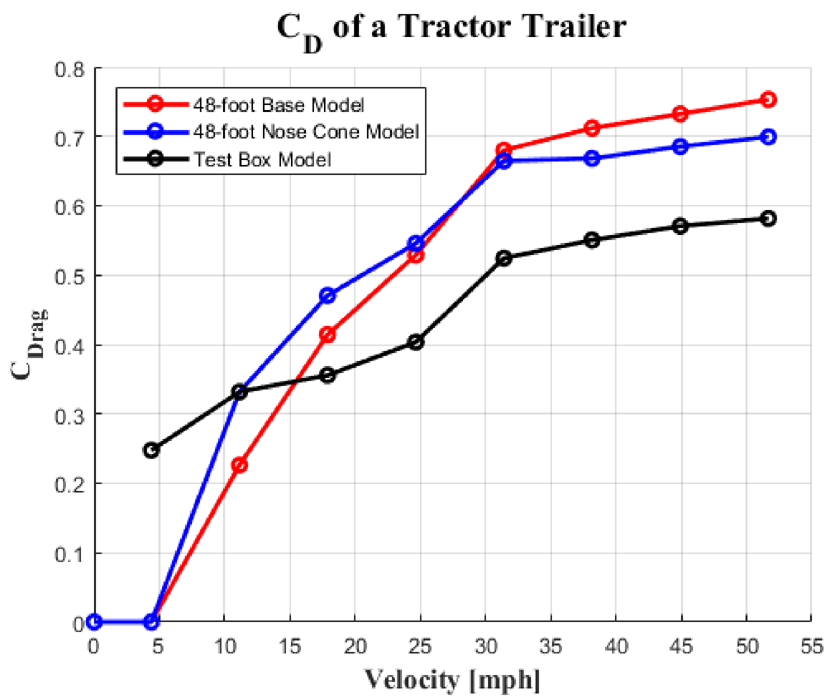

Figure 43. Preliminary testing results with a 48-foot trailer and a short test box.

Data Reduction Techniques

We ran each configuration twice in the wind tunnel and recorded the drag force values in Excel. We then averaged the values obtained from each trial at each recorded frequency to reduce the amount of error. To calculate the correct velocity of air in the wind tunnel, a correlation given in the wind tunnel manual relates the air velocity, V, to the wind tunnel motor frequency, f, by using the following equation: [3]

$$V = 1.2081f - 1.0632 \quad (1)$$

This first equation models the velocity as a linear relationship because the frequency ratio of the air velocity to the motor frequency was roughly 1:1. The drag coefficient, C_D, was found by

$$C_D = \frac{2*F_D}{(\rho*A*V^2)} \quad (2)$$

where F_D is the drag force, ρ is the density of air, V is the velocity of air, and A is the cross-sectional area of our model. [4] This equation gave us the necessary information to construct the plots (see Appendix A) for each trailer configuration and later allowed us to calculate the CO_2 emissions output (in grams of CO_2/ton-mile) and our fuel consumption rates (in gallons of diesel/1000 ton-mile). The CO_2 emissions output equation is stated: [5]

$$e_{CO2} = (C_1 + C_2 * TRRL + C_3 * \Delta C_D A + C_4 * WR) * C_5 \quad (3)$$

Constants C_1 through C_4 deal with whether the trailer is a long dry box van or a short dry box van (Figure 14). Tire Rolling Resistance (TRRL) and Weight Reduction (WR) values were taken from an example from Cornell Law School that discussed the details of the new regulations. [1] $\Delta C_D A$ is the change in the drag coefficient multiplied by the front cross-sectional area of the model, which is referred to as a change in drag area. Lastly, C_5 is a constant that accounts for specific tire pressure systems (1.0 for no system installed).

Trailer Category	C_1	C_2	C_3	C_4
Long dry box van	76.1	1.67	-5.82	-0.00103
Long refrigerated box van	77.4	1.75	-5.78	-0.00103
Short dry box van	117.8	1.78	-9.48	-0.00258
Short refrigerated box van	121.1	1.88	-9.36	0.00264

Constant	Value
TRRL	4.6
A (in²) – 48'	8.013
A (in²) – A-Train	5.219
WR	655
C_5	1.00

Figure 14. Trailer Category and Constant Values

After the CO_2 emissions output were calculated, we could find the fuel consumption rates, FC. This equation is as follows: [5]

$$FC\left(\frac{gal_{Diesel}}{1000ton{-}mile}\right) = \frac{e_{CO2}\left(\frac{g_{CO2}}{ton{-}mile}\right)}{10{,}180\left(\frac{g_{CO2}}{gal_{Diesel}}\right)} * 1000 \quad (4)$$

10,180 grams of CO_2 are in one gallon of diesel, hence this conversion factor in the denominator. The emissions output is also multiplied by 1,000 to account for the 1,000 ton-miles travelled for the fuel consumption rates.

Test Results

Appendix A contains all the drag coefficient plots that were obtained from testing our model trailers in the University of Idaho's wind tunnel. Below are quick summaries of our results for the 48-foot and 53-foot trailers as well as the A-Train trailers.

48-foot and 53-foot Trailer Results

We saw that changing the front-end attachments from nothing to a nose cone and then to a bull nose caused significant reductions in the drag coefficient. Figure 15 shows this trend with no under-carriage configuration. The worst drag coefficient we calculated for the 48-foot and 53-foot models was the 48-foot base model, which has no front-end nor under-carriage configuration. That drag coefficient was 0.704. Adding a nose cone caused in a reduction of

7.5% resulting in a drag coefficient of 0.652. A bull nose reduced the drag coefficient by almost 21% giving a value of 0.557.

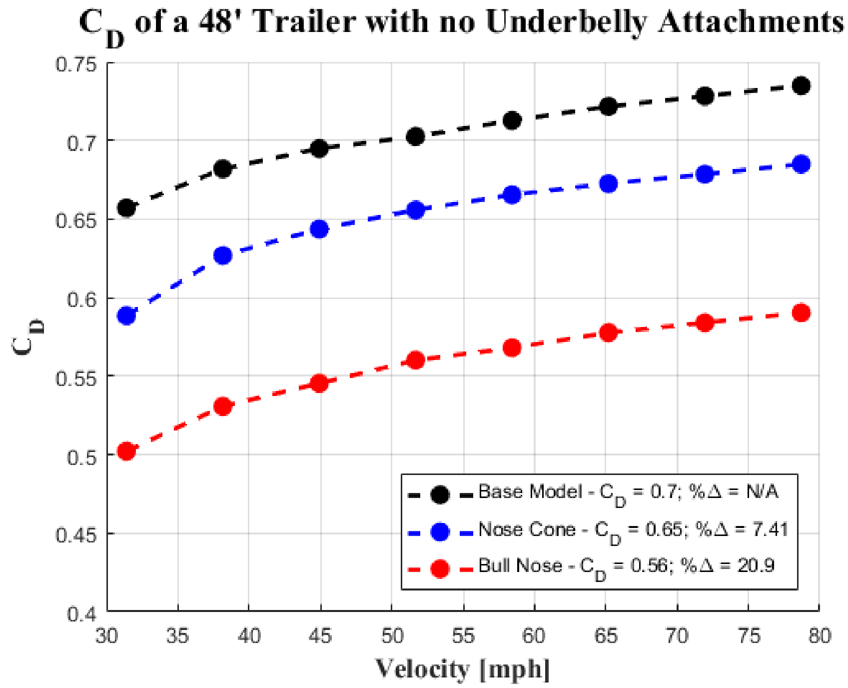

Figure 15. Drag coefficient against velocity for the three different front-end configurations.

Changing the under-carriage configuration from nothing to hopper bins and then to a possum belly also saw substantial reductions in the drag coefficient, but not as significant as the front-end results. These tests in Figure 16 were done with no front-end configuration. Adding hopper bins to the trailer gave a drag coefficient of 0.681, about a 3% change from the 48-foot base

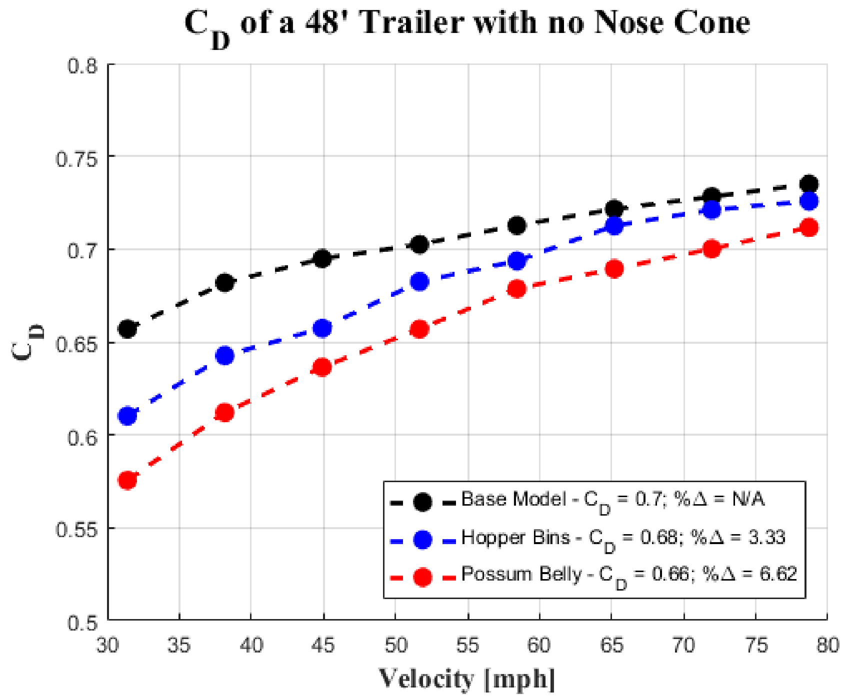

Figure 16. Drag coefficient against velocity for the three different under-carriage configurations.

model. A possum belly configuration gave a drag coefficient of 0.658 which is about a 6% change.

A-Train Trailer Results

For the A-Train Trailers, we saw that adding a nose cone to both the lead and pup trailers provided a significant decrease in the drag coefficient across all tongue lengths. The tests that were ran without a nose cone all followed closely to a common linear trend at higher speeds, whereas the tests done with a nose cone saw larger deviations from one another. We assumed the wider spread of data for the A-Train trailers with nose cones is due to either added turbulence from the shape of the nose cones or slight sensor errors in the wind tunnel.

Figure 17 shows five drag coefficient trends for the five different tongue lengths. At lower speeds, the data between each tongue lengths has a large spread of drag coefficients, but as the velocity increases, all tongue lengths converged closely to a single linear trend. The A-Train trailer configuration that saw the highest drag coefficient was the longest tongue length (21-foot 7-inch) without a nose cone. Its average drag coefficient was 0.918. The relative change in drag coefficient for the models with and without a nose cone were calculated from the model with the shortest length, which is why the longest length without a nose cone saw a negative change in drag coefficient, about -2.7%.

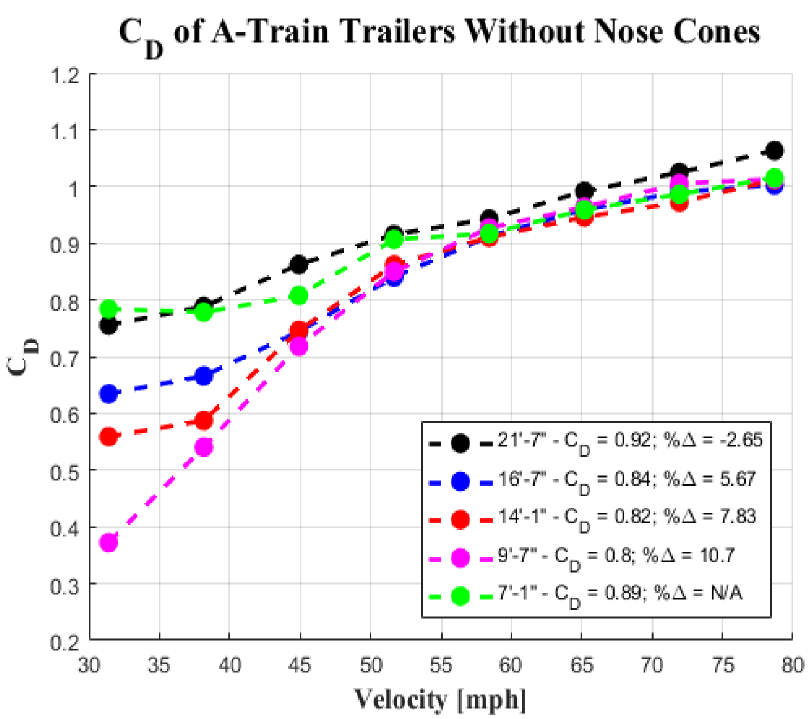

Figure 17. Drag coefficients for every possible A-Train trailer tongue length without nose cones.

Tests done on the A-Train trailers with nose cones can be seen in Figure 18. For these tests, the shortest trailer produced the largest drag coefficient at 0.799. A tongue length of 9-foot 7-inches saw a reduction of about 25% in the drag coefficient, producing the lowest drag coefficient value out of all A-Train models tested, which was 0.601.

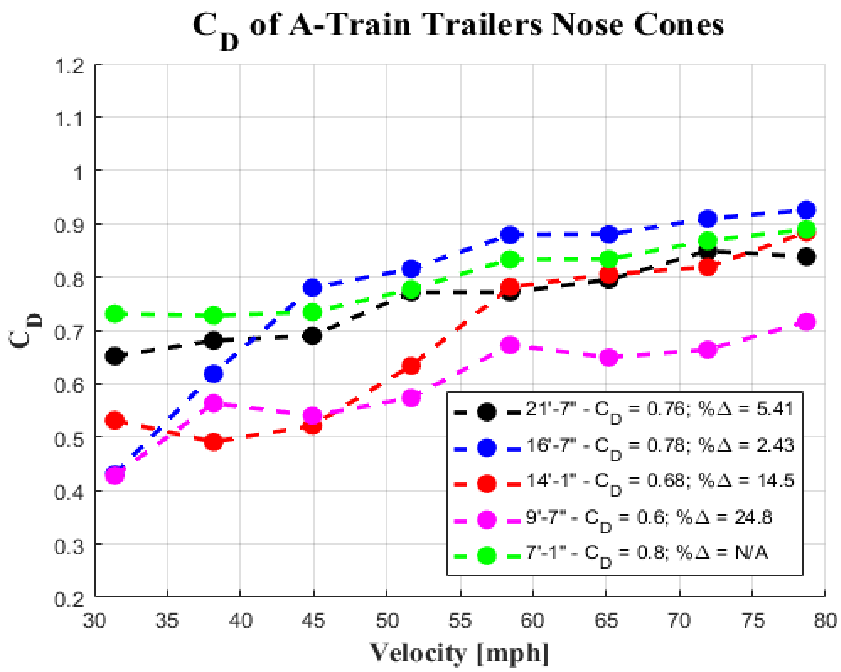

Figure 58. Drag coefficients for every possible A-Train trailer tongue length with nose cones.

Error Analysis

On top of the drag coefficient plots, we performed an error analysis on all the data to ensure a reduction in drag coefficients can be concluded. The root-sum-square method was used on Equation 2 with each variable having its own uncertainty. The drag force uncertainty was 0.00454N [3], the velocity uncertainty was 1 m/s, the density uncertainty was 0.0001 kg/m^3, and

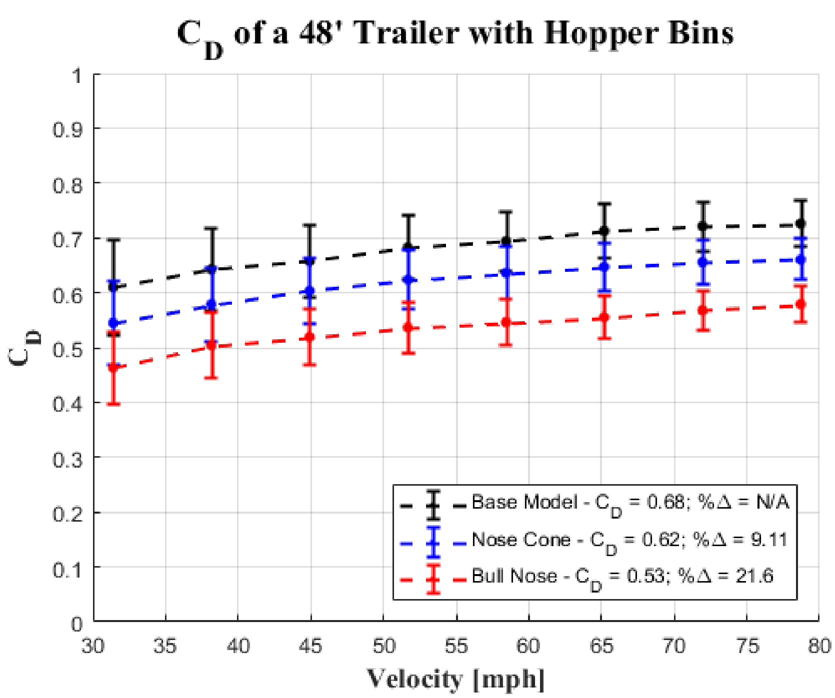

Figure 19. Error analysis for drag coefficients of a 48-foot trailer with hopper bins.

the area uncertainty was 0.00001 m^2. Figures 19 and 20 show some drag coefficient plots with error bars for a single trailer and A-Train trailer setup, respectively.

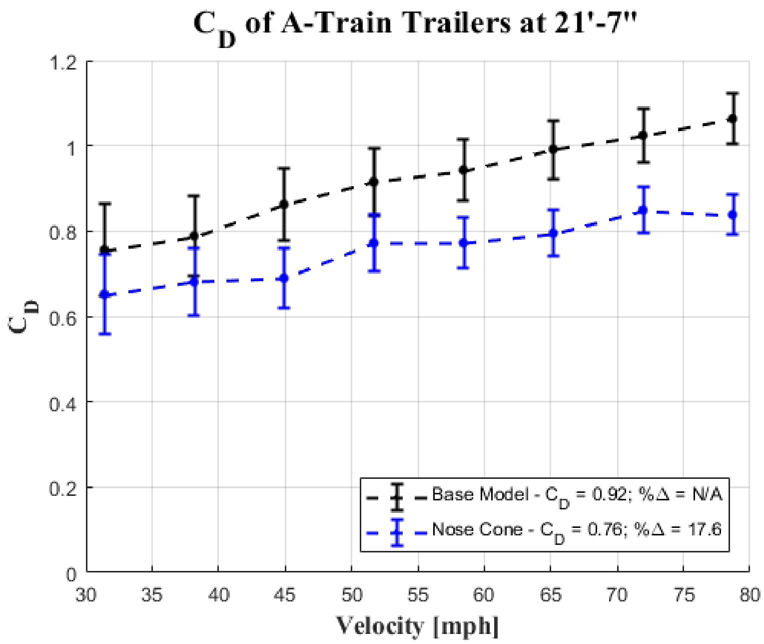

Figure 20. Error analysis for drag coefficients of an A-Trail trailer at the longest tongue length.

In both Figures, we can see that there is no conclusive evidence that the drag coefficient reduces at lower speeds due to the error bars overlapping. As the speed increases, however, the error bars begin to diverge and eventually separate, indicating that the drag coefficient did reduce between the trailer models.

Emissions Predictions

After the drag coefficients were determined for each model configuration tested, we calculated the corresponding emissions output for each model, which was done using Equation 3. The only variable we focused on was the change in drag area, $\Delta C_D A$. All other variables were held constant. Since this value is based on a change in drag coefficient, the models that produced the highest drag coefficient for the single trailers and A-Train trailers did not have an emissions output nor a fuel consumption rate. Table 4 gives the emissions output values calculated for each model.

Table 4. Emissions output for all trailer models tested.

Emissions Output (g-CO2/ton-mile)					
48-foot Trailer			**A-Train Trailer**		
No Nose Cone	No Under-Carriage	N/A	**No Nose Cone**	7'-1"	123.2
	Hopper Bins	122.7		9'-7"	118.7
	Possum Belly	81.1		14'-1"	119.9
Nose Cone	No Under-Carriage	120.7		16'-7"	120.8
	Hopper Bins	118.4		21'-7"	N/A
	Possum Belly	78.5	**Nose Cone**	7'-1"	118.7
Bull Nose	No Under-Carriage	114.2		9'-7"	109.4
	Hopper Bins	112.6		14'-1"	113.3
	Possum Belly	74.7		16'-7"	117.8
				21'-7"	116.7

Table 1 gives the regulations for emissions output for current and future model years. The maximum output for short, dry trailers is 125.4 g-CO_2/ton-mile, and the maximum output for long, dry trailers is 81.3 g-CO_2/ton-mile.

Fuel Consumption Rates

The emissions output values were then used to find each trailer's respective fuel consumption rates using Equation 4. Since this value depends on the emissions output, and the emissions output depends on a change in drag coefficient, the models that produced the highest drag coefficients did not have a calculated fuel consumption rate. Table 5 shows the rates for all possible models.

Table 5. Fuel consumption rates for all trailer models tested.

Fuel Consumption Rates (Gal-diesel/1000 ton-miles)					
48-foot Trailer			**A-Train Trailer**		
No Nose Cone	No Under-Carriage	N/A	**No Nose Cone**	7'-1"	12.10080
	Hopper Bins	12.05120		9'-7"	11.65970
	Possum Belly	7.97010		14'-1"	11.77800
Nose Cone	No Under-Carriage	11.85640		16'-7"	11.86700
	Hopper Bins	11.63150		21'-7"	N/A
	Possum Belly	7.71150	**Nose Cone**	7'-1"	11.66310
Bull Nose	No Under-Carriage	11.21530		9'-7"	10.74780
	Hopper Bins	11.05710		14'-1"	11.12840
	Possum Belly	7.34110		16'-7"	11.57360
				21'-7"	11.46340

Table 2 gives the current regulations for fuel consumption rates on models made between 2018 and 2020, as well as regulations for future years. Currently, the maximum rate for short, dry trailers is 12.318 gallons of diesel per 1000 ton-miles. The maximum rate for long, dry trailers is 7.986 gallons of diesel per 1000 ton-miles.

Conclusions

From our data analysis, the 53-foot trailer with a possum belly and nose cone (Figure 21) has the lowest drag coefficient out of the 48-foot and 53-foot trailer models, resulting in the lowest emissions output of 74.7 g-CO_2/ton-mile and lowest fuel consumption rate of 7.341 gallons of diesel/1000 ton-mile. The resulting fuel savings is about 39% from the base model.

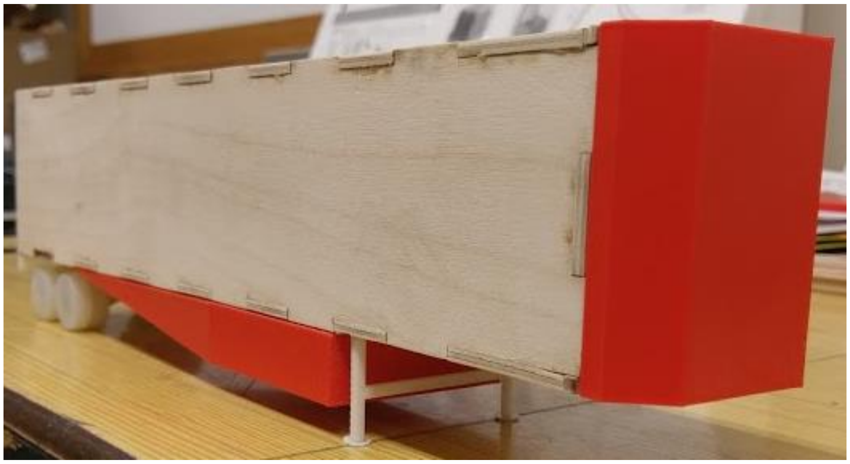

Figure 21. The best Single Trailer configuration arose from applying a bull nose attachment and a possum belly attachment.

The A-Train trailer with the 9-foot, 7-inch tongue length (Figure 22) produced the lowest drag coefficient out of all the possible A-Train lengths, resulting in the lowest emissions output of 109.4 g-CO_2/ton-mile and lowest fuel consumption rate of 10.747 gallons of diesel/1000 ton-mile. About 11% in fuel savings is achieved with the best A-Train setup, compared to the A-Train base model.

Figure 22. The best A-Train configuration resulted from applying a nose cone to both trailers with a tongue length distance of 9'7".

These emissions output and fuel consumption rates for both the single and A-Train trailers meet current EPA requirements for the 2018-2020 model years (see Tables 1 and 2), but changes will need to be made on the trailers, aerodynamically or otherwise, to meet future regulations.

The average 4-door passenger vehicles gets about 22 miles per gallon, [6] whereas the average semi-truck gets roughly 6 miles per gallon. [2] Because of this wide difference in fuel economy, the aerodynamics of the trucking industry require more attention for improvement to reduce emissions and fuel consumption.

Future Recommendations

We recommend a skin friction drag analysis for our models, as the balsa wood used to construct them has a different texture than typical sheet metal used to construct full-size trailers (Figure 23). We are unsure how significant the skin friction drag played in our aerodynamic drag tests, but it would be good to ensure that is does not significantly affect the data.

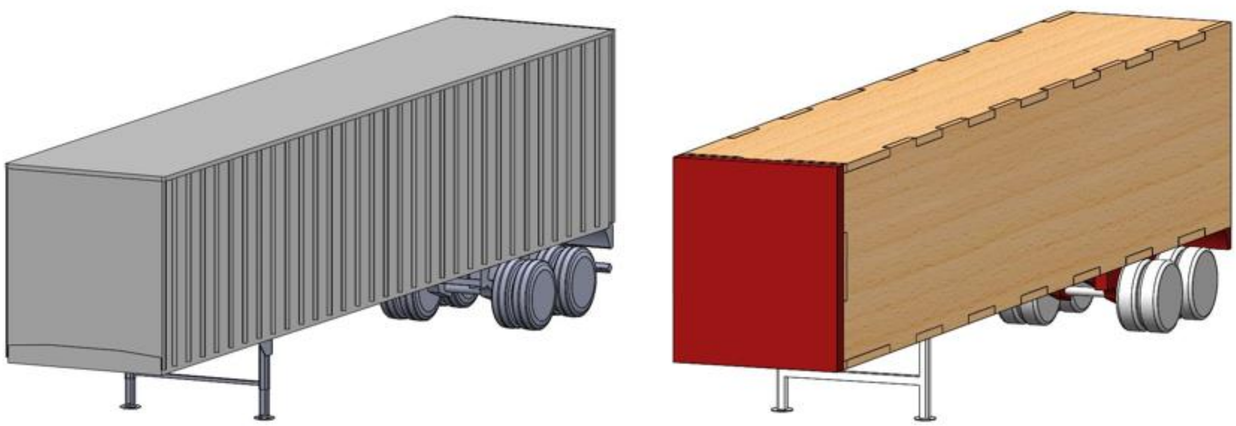

Figure 23. Comparing a full-size trailer side panel and the model side panels.

We also recommend an analysis with a semi-truck in front of the trailers, as we expected the nose cone front-end configuration on the 48-foot trailer to have a lower drag coefficient than a bull nose configuration. This is because the nose cone attachments have an underside to the rounded top, creating a possible pocket of stagnant, high-pressure air. If a semi-truck were in front of the trailers, this area would be shrouded by the truck and potentially decreasing the aerodynamic drag.

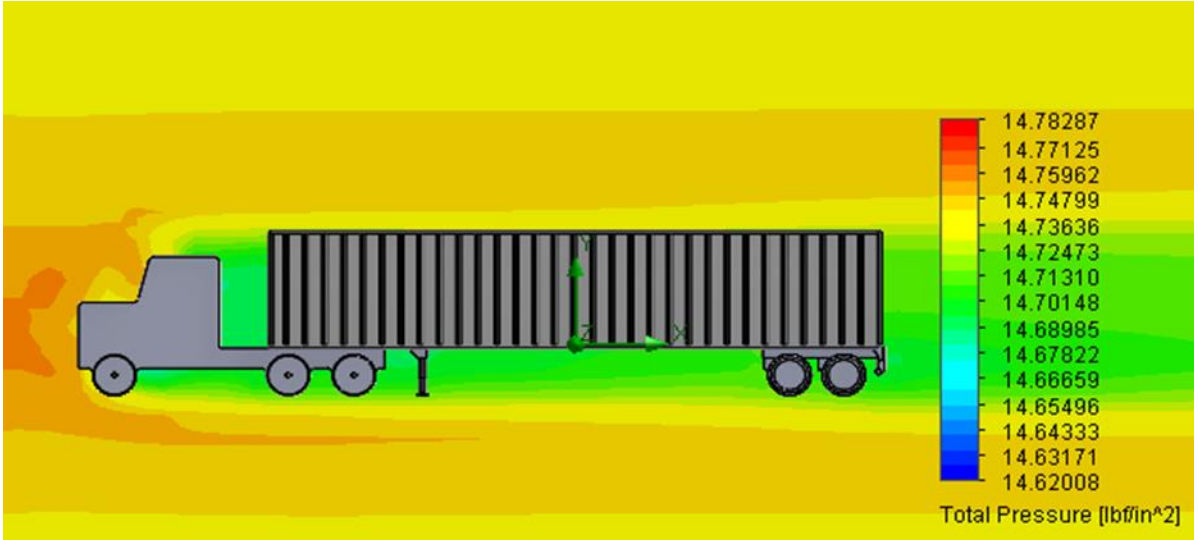

Figure 24. A simple Computational Fluid Dynamics analysis of the single trailer base model with a truck in front.

From the CFD analysis in Figure 24, a low-pressure zone exists between the front of the trailer and the back side of the cab of the truck, typically where a nose cone attachment would be placed. Without a truck in front of a nose cone, a high-pressure zone would form on the underside of the nose cone, which could create drag forces that are not usually present when a bulk commodity tractor trailer is being towed.

References

[1] "40 CFR Part 1037 - CONTROL OF EMISSIONS FROM NEW HEAVY-DUTY MOTOR VEHICLES." LII / Legal Information Institute, Environmental Protection Agency, www.law.cornell.edu/cfr/text/40/part-1037.

[2] Berg, Phil. "10 Things You Didn't Know About Semi Trucks." *Popular Mechanics*, Hearst Communications, Inc, 14 Nov. 2017, www.popularmechanics.com/cars/trucks/g116/10-things-you-didnt-know-about-semi-trucks/.

[3] Cunnington, Matthew J., Westra, Levi J., Beyerlein, Steven W., Budwig, Ralph S., and Donald F. Elger, "Design of a Wind Tunnel Facility for Hands-on Use by Beginning Engineering Students," *University of Idaho Mechanical Engineering Department*, Moscow, ID, 2002.

[4] D. F. Elger, B. C. Williams, C. T. Crowe and J. A. Roberson, Engineering Fluid Mechanics, 10th Ed., John Wiley & Sons, Inc., 2013.

[5] "Phase 2 Heavy-Duty Greenhouse Gas (GHG) and Fuel Consumption," in Trailer Implementation Workshop, Ann Arbor, 2016.

[6] Staff, Cars.com. "Best and Worst Gas Mileage 2016 | News from Cars.com." *Cars.com*, Cars.com, 8 Feb. 2016, www.cars.com/articles/best-and-worst-gas-mileage-2016-1420683223195/.

[7] "Wind Tunnel Facility." Influence of Electronic Media on Reading Ability of School Children, J.C. Igbokwe, N.A. Obidike, E.C. Ezeji, University of Idaho Mechanical Engineering Department, www.webpages.uidaho.edu/fluidslab/Fluids/WindTunnel/wind_tunnel_facility.htm.

Appendices

Appendix A

Drag coefficient plots

Part 1: 48-foot and 53-foot trailer configuration plots

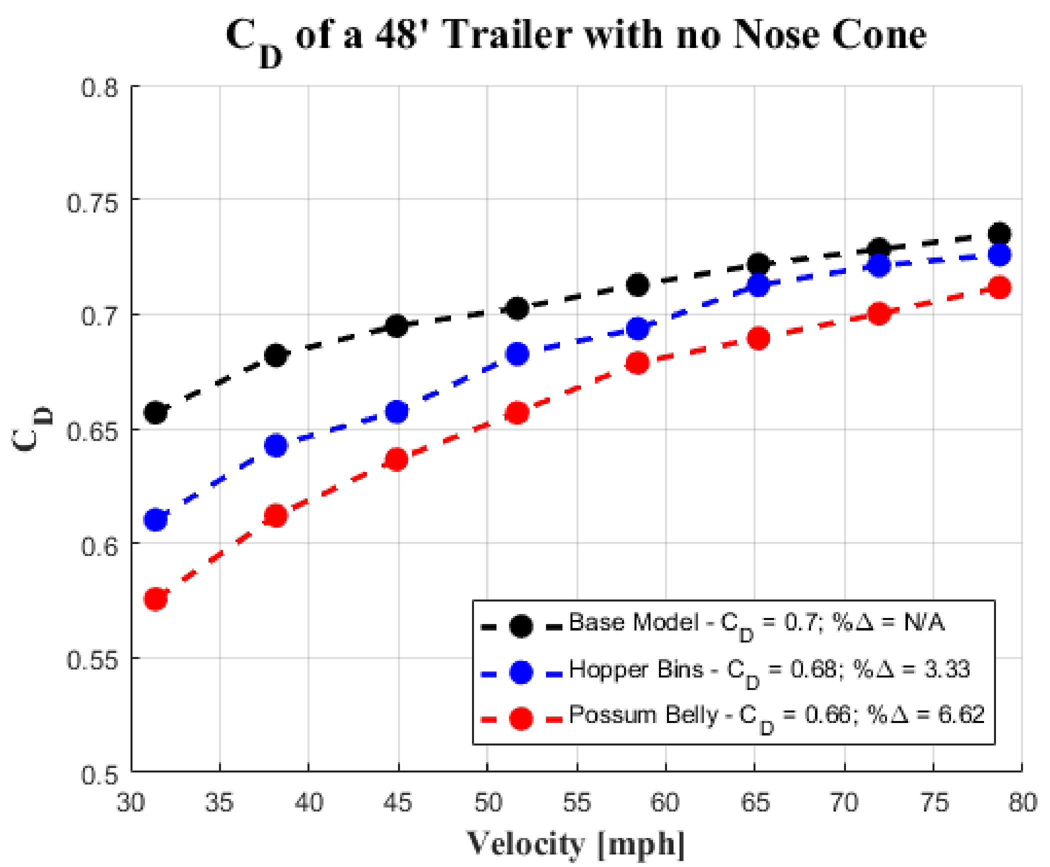

Figure A1.1

Drag coefficient plotted against velocity for a 48-foot and 53-foot trailer without a nose cone while altering the under-carriage configuration.

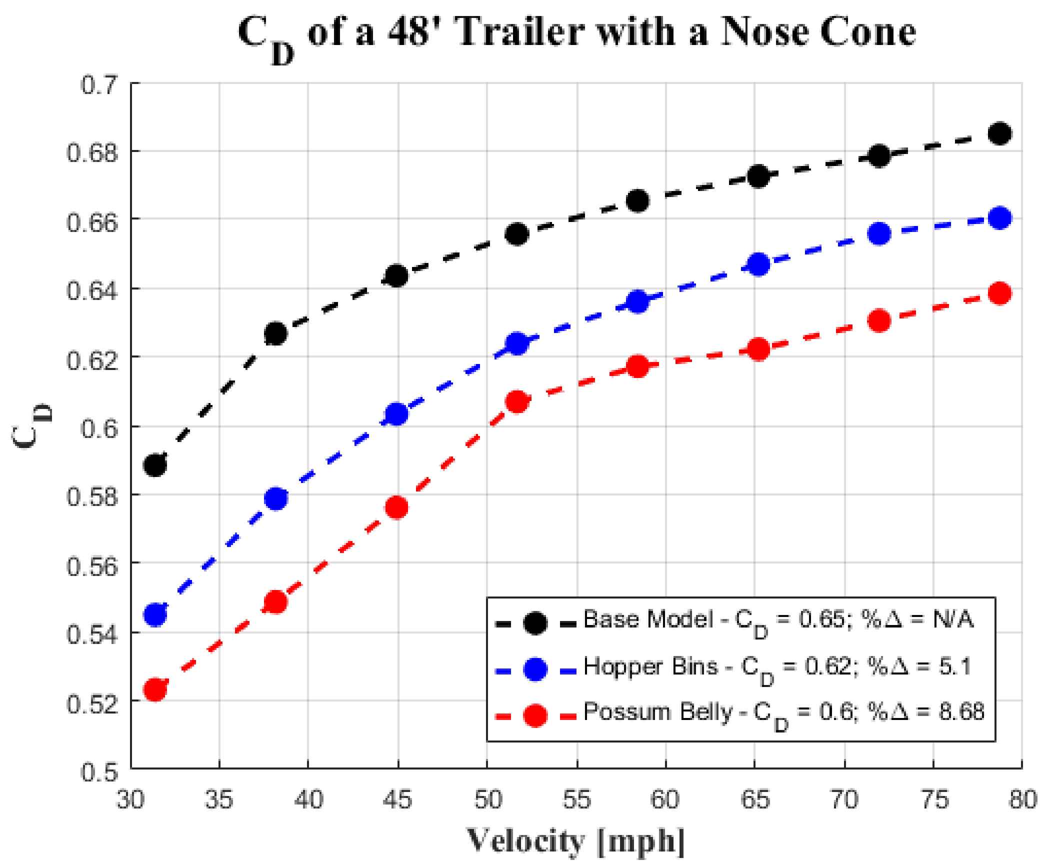

Figure A1.2
Drag coefficient plotted against velocity for a 48-foot and 53-foot trailer with a nose cone while altering the under-carriage configuration.

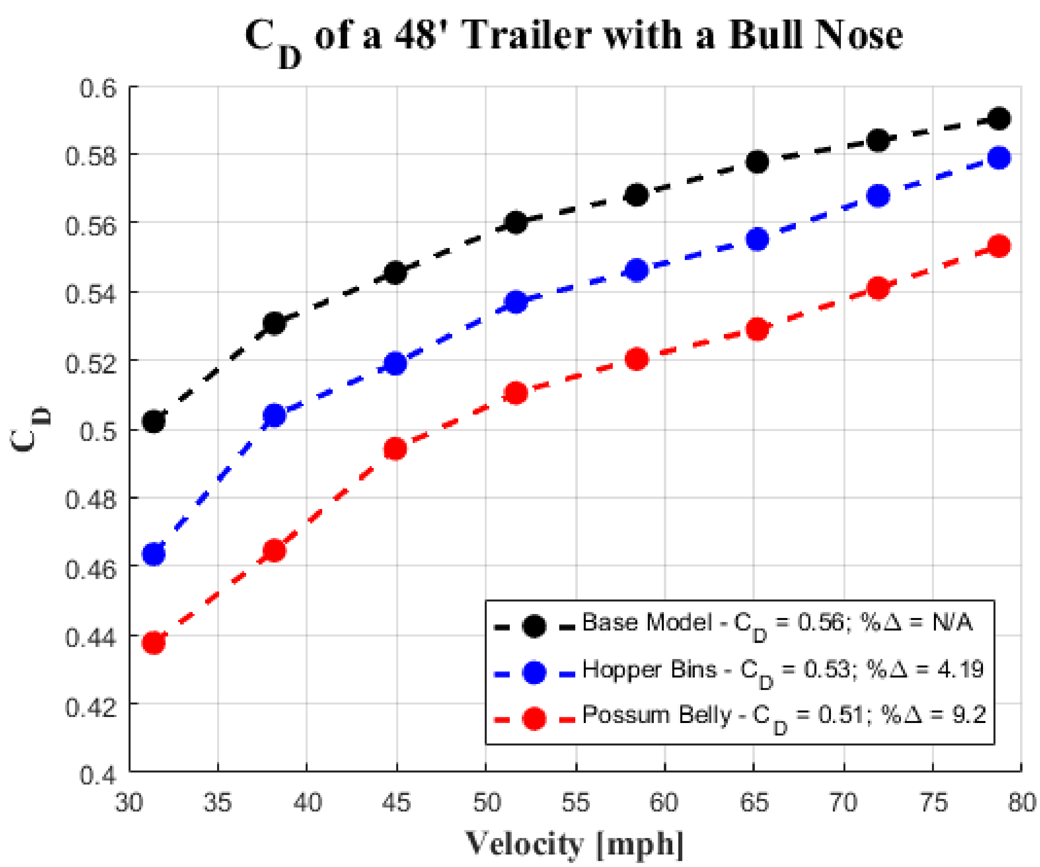

Figure A1.3
Drag coefficient plotted against velocity for a 48-foot and 53-foot trailer with a bull nose while altering the under-carriage configuration.

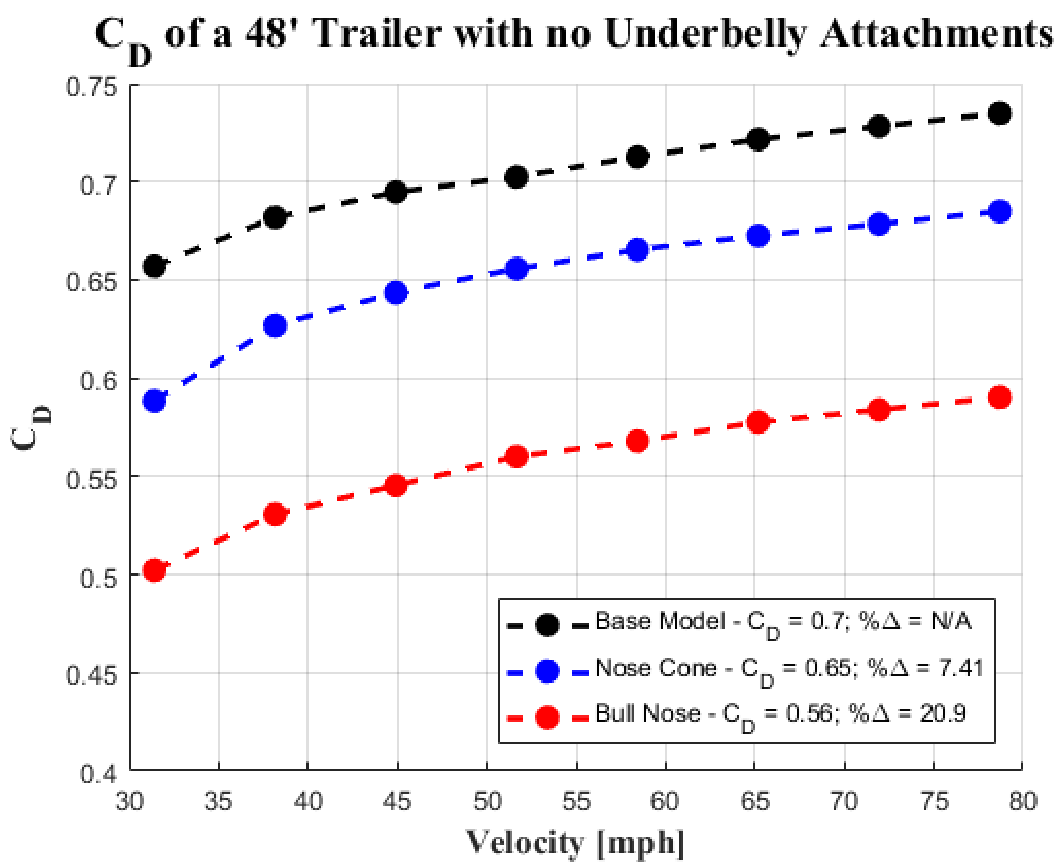

Figure A1.4
Drag coefficient plotted against velocity for a 48-foot trailer without an under-carriage attachment while altering the front end of the trailer.

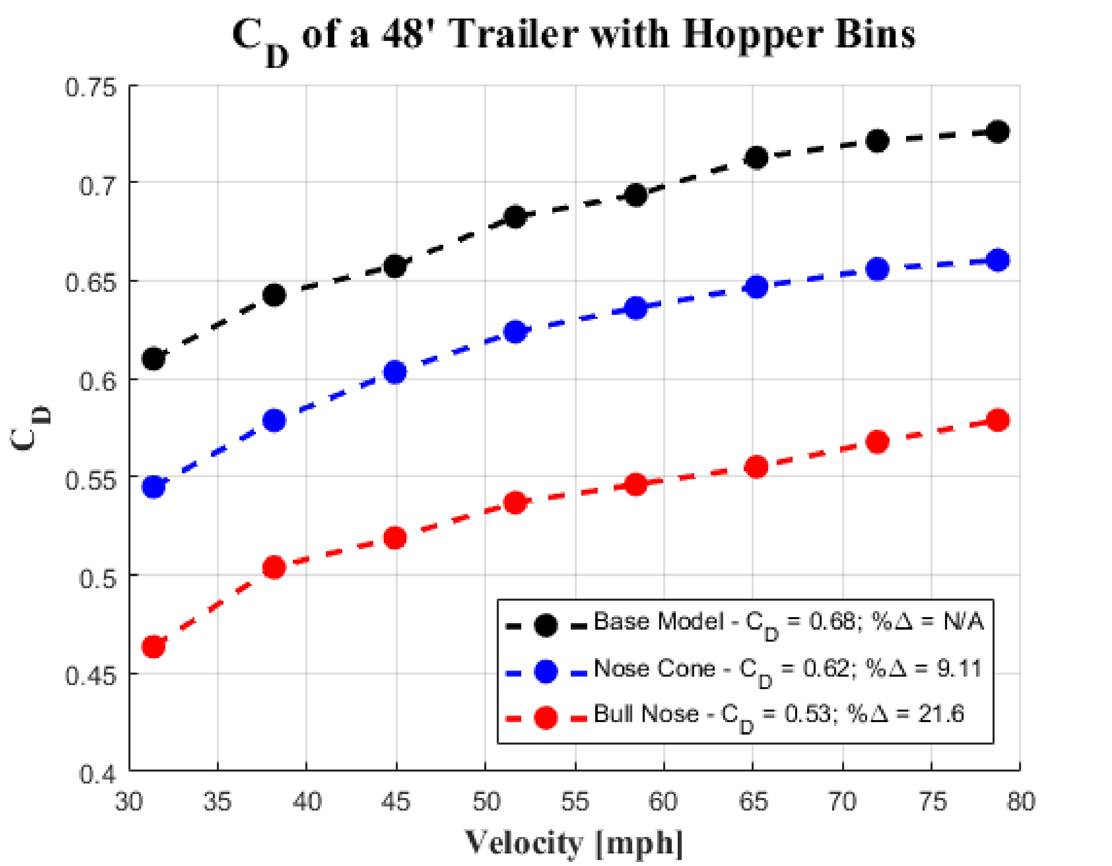

Figure A1.5
Drag coefficient plotted against velocity for a 48-foot trailer with hopper bins attached while altering the front end of the trailer.

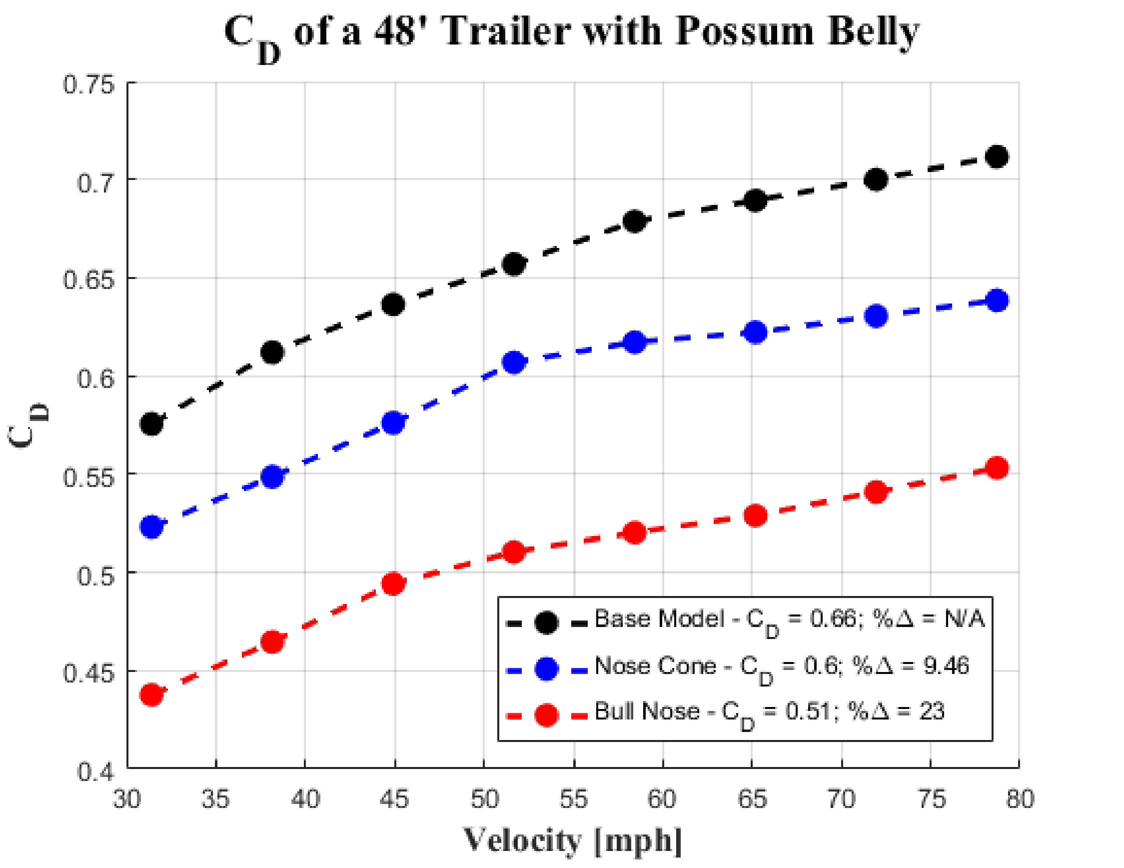

Figure A1.6
Drag coefficient plotted against velocity for a 53-foot trailer with a possum belly attached while altering the front end of the trailer.

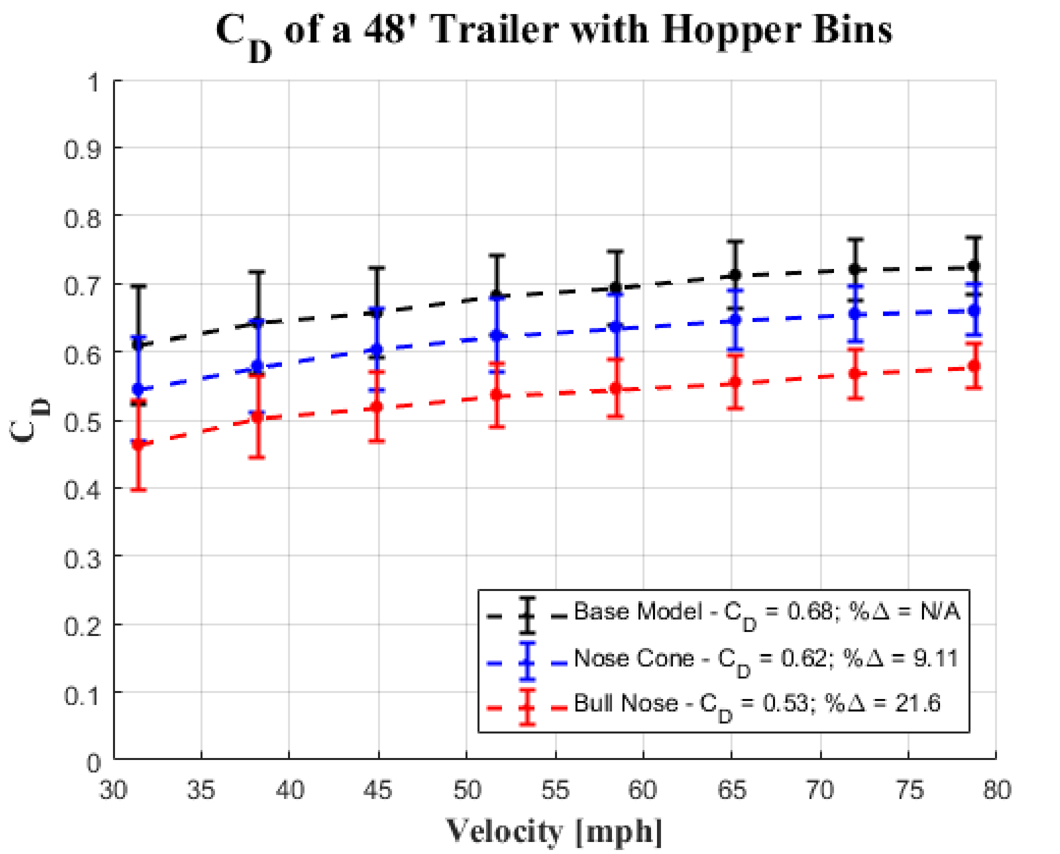

Figure A1.7
Drag coefficient plotted against velocity with an error analysis for a 48-foot trailer with a hopper bins attached while altering the front end of the trailer.

Part 2: A-Train configuration plots

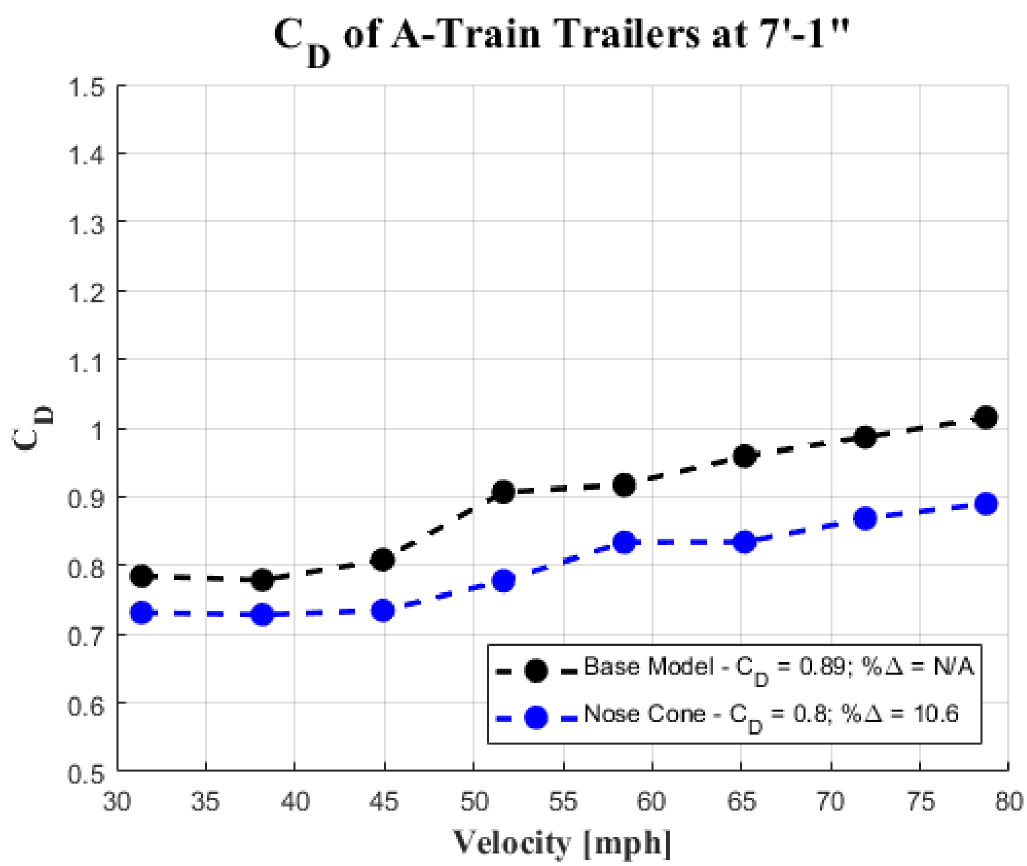

Figure A2.1
Drag coefficient plotted against velocity for the A-Train trailer tongue length of 7-foot 1-inch with and without a nose cone.

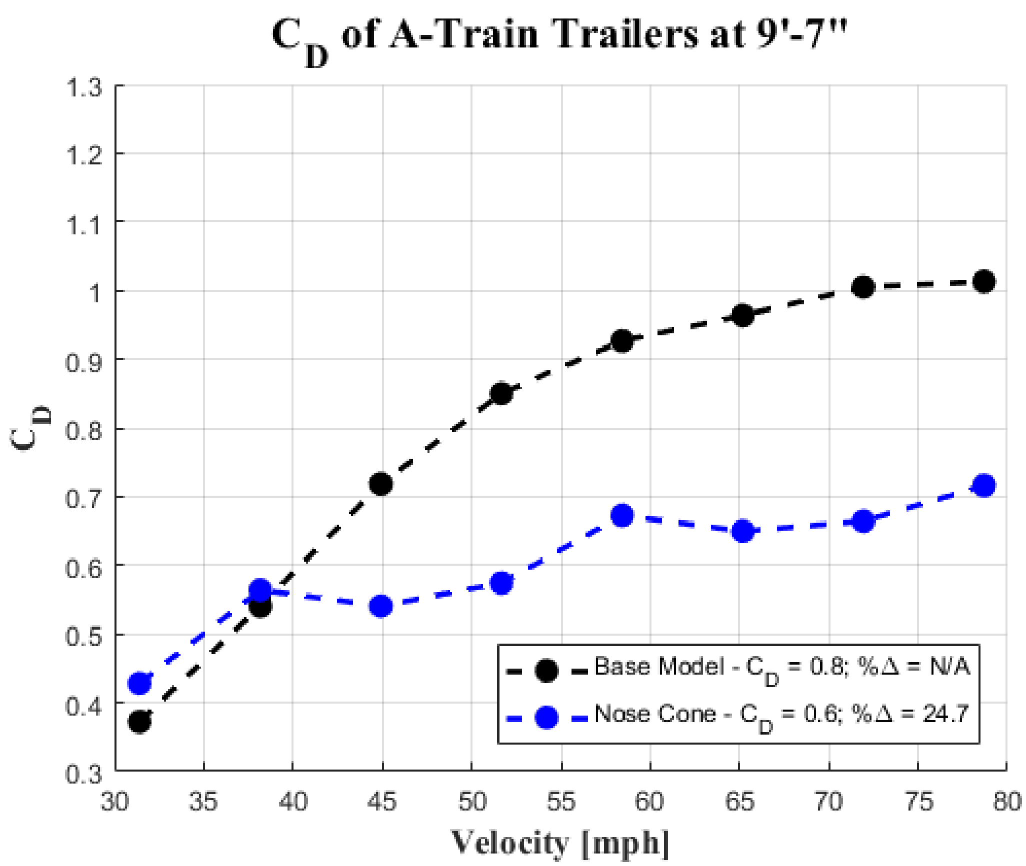

Figure A2.2
Drag coefficient plotted against velocity for the A-Train trailer tongue length of 9-foot 7-inch with and without a nose cone.

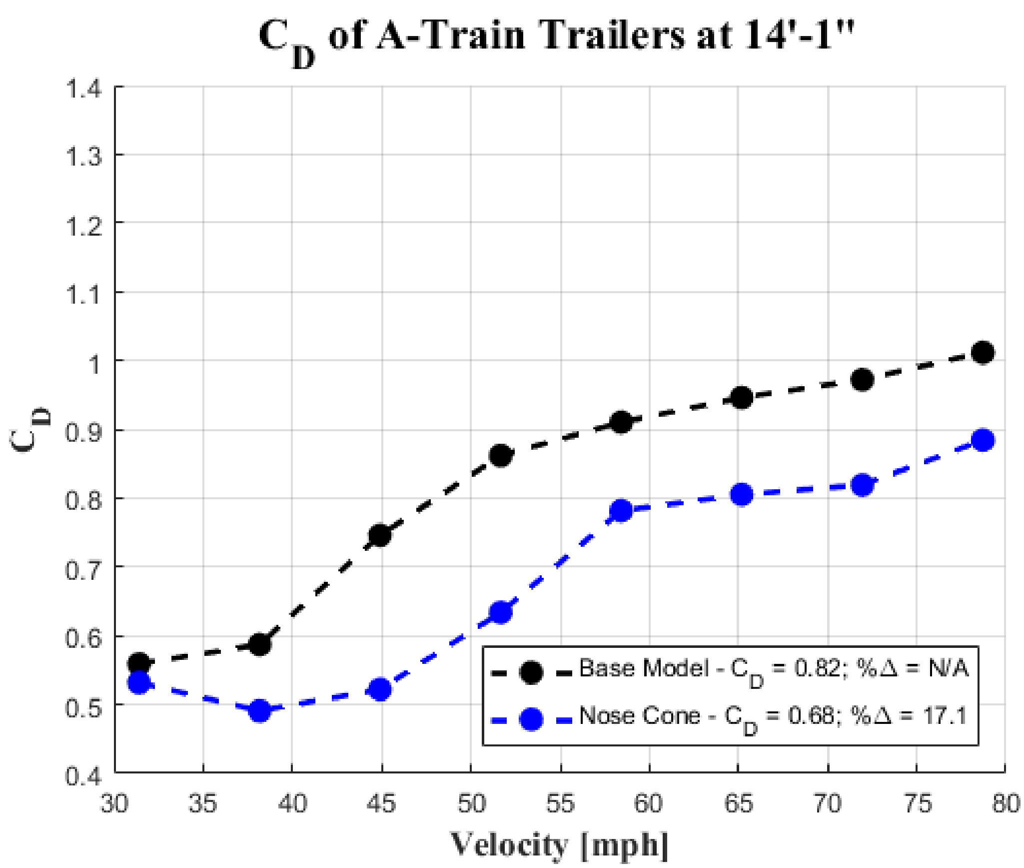

Figure A2.3
Drag coefficient plotted against velocity for the A-Train trailer tongue length of 14-foot 1-inch with and without a nose cone.

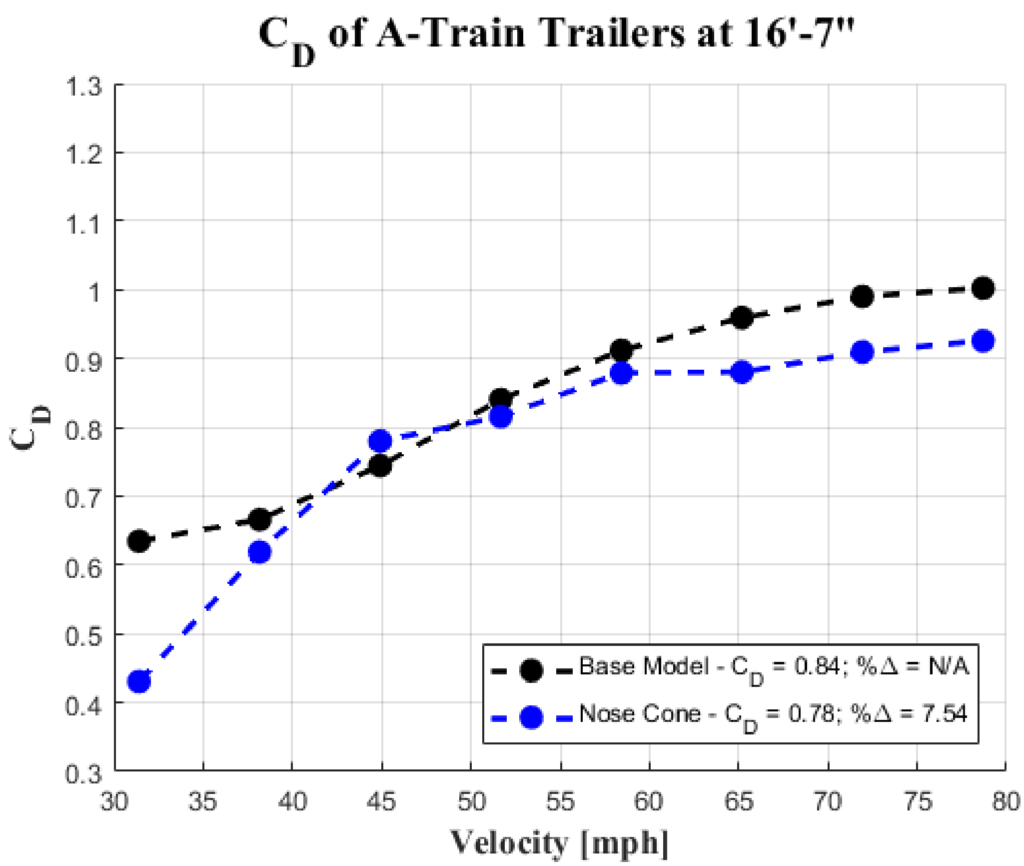

Figure A2.4
Drag coefficient plotted against velocity for the A-Train trailer tongue length of 16-foot 7-inch with and without a nose cone.

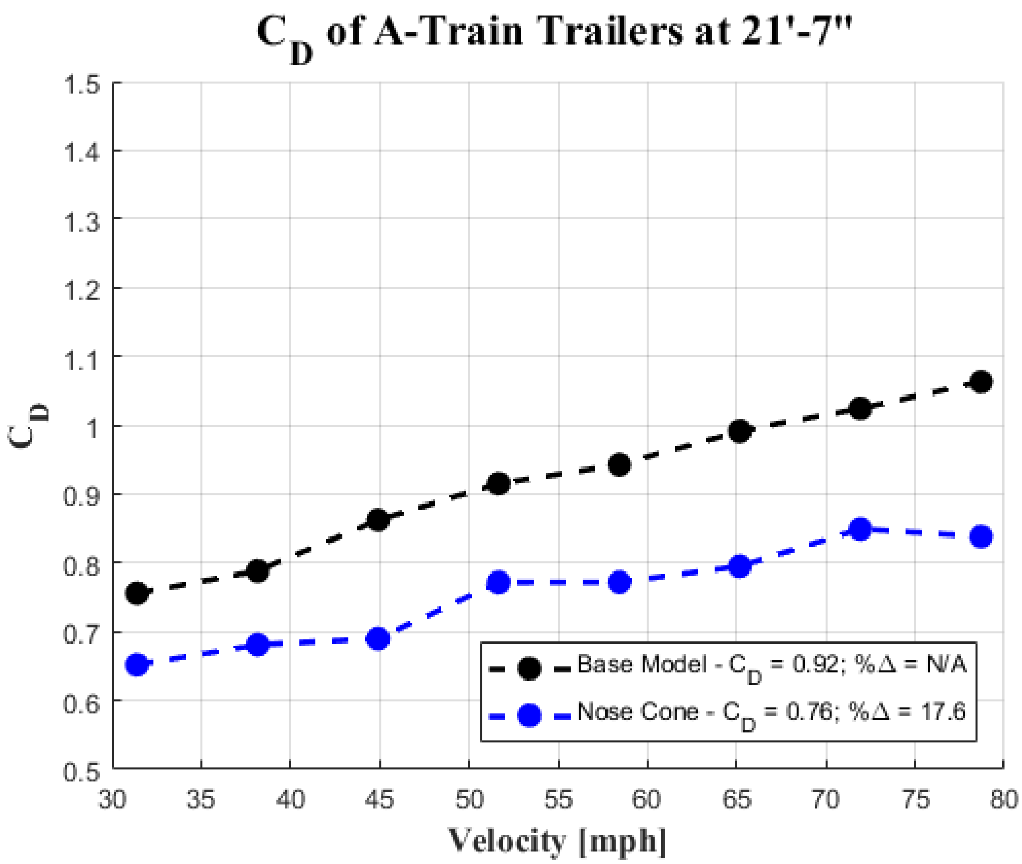

Figure A2.5
Drag coefficient plotted against velocity for the A-Train trailer tongue length of 21-foot 7-inch with and without a nose cone.

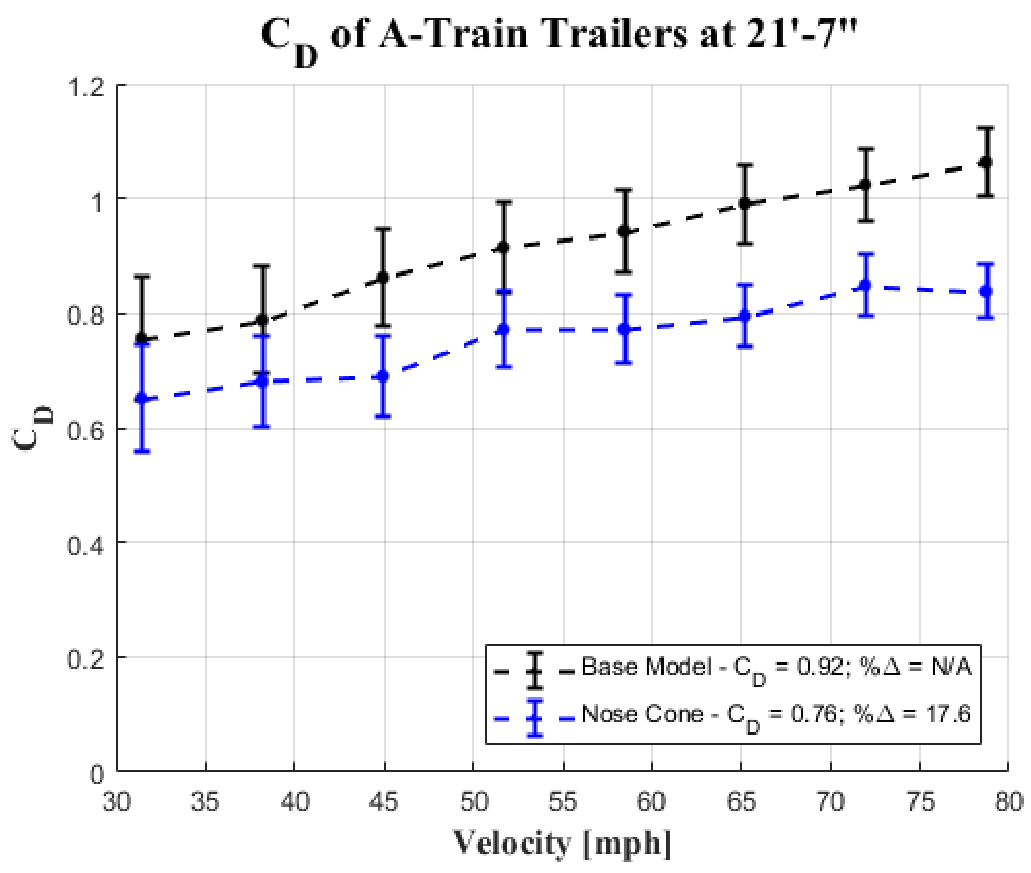

Figure A2.6
Drag coefficient plotted against velocity for the A-Train trailer tongue length of 21-foot 7-inch, with and without a nose cone and including an error analysis.

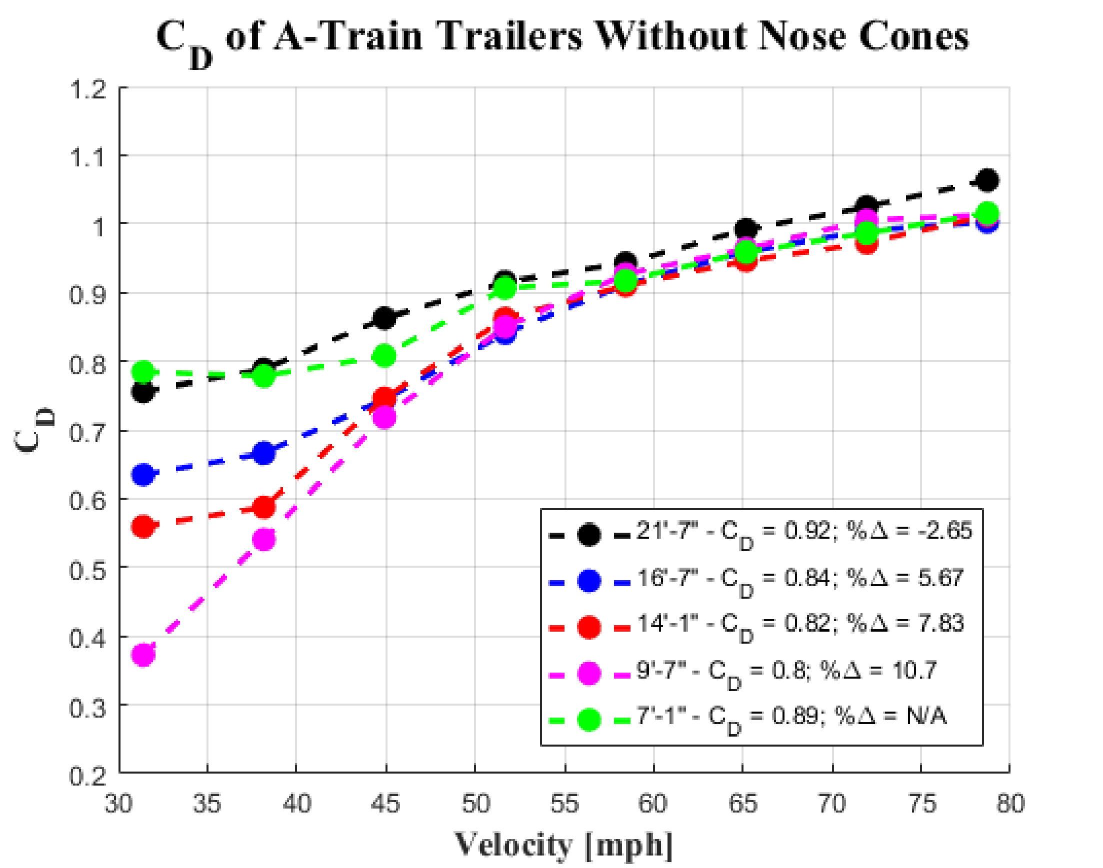

Figure A2.7

Drag coefficient plotted against velocity for the A-Train trailer without a nose cone and all tongue lengths.

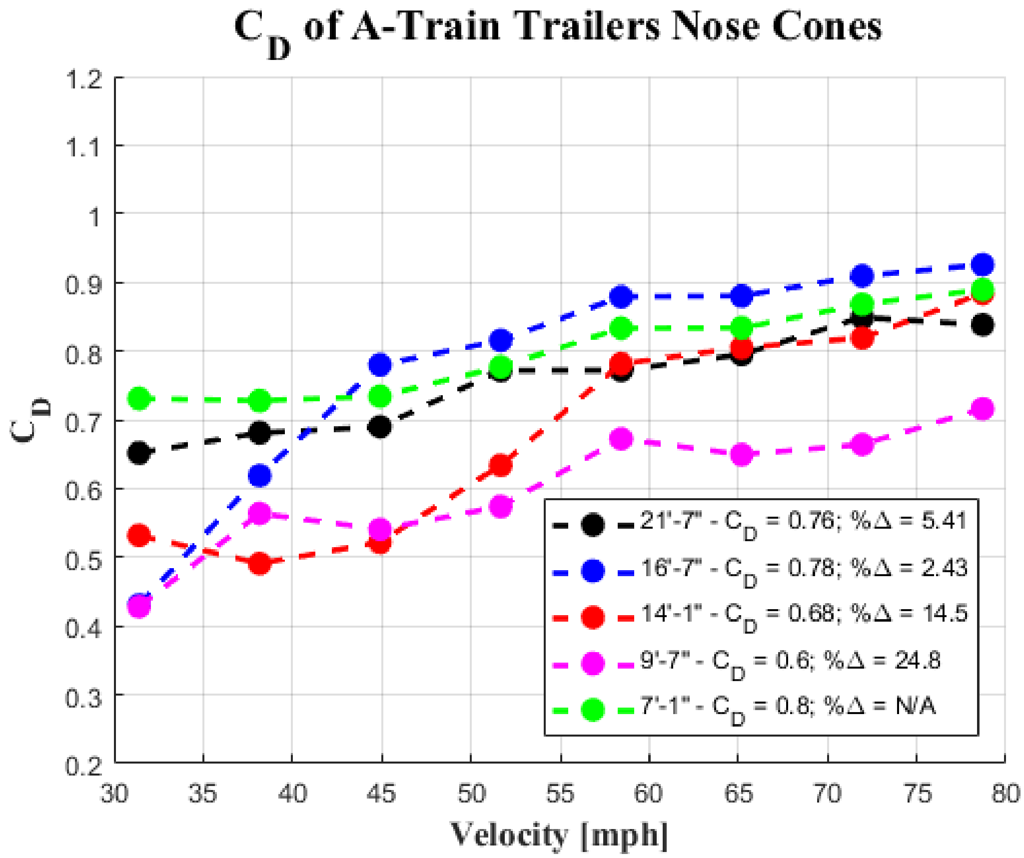

Figure A2.8
Drag coefficient plotted against velocity for the A-Train trailer with a nose cone and all tongue lengths.

<u>Appendix B</u>

Wind tunnel Setup Procedure

Step	Description	Image
1	Turn on the digital circuitry housing and tare the readouts to read zero. **Note**: Do this first to ensure enough time to warm up. Warm up time is approximately 15 minutes.	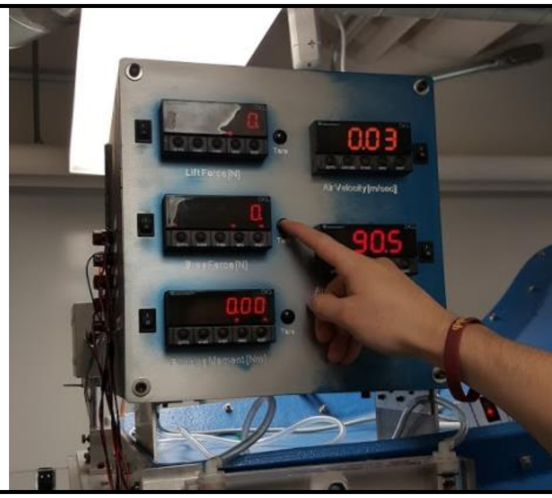
2	Remove lid and fasten male force balance attachment by tightening the set screw.	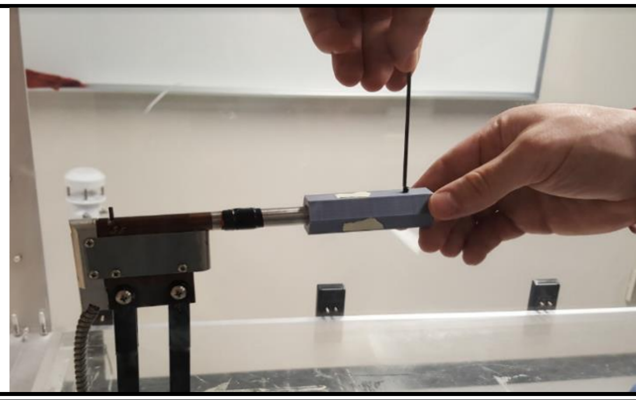
3	Mount the trailer on the force balance in the normal position shown.	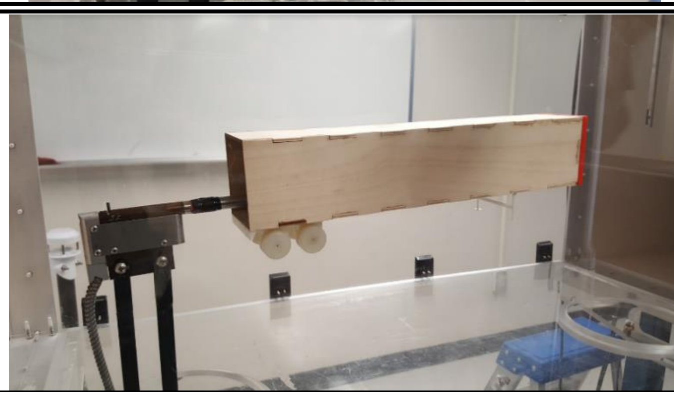

4	Place airfoil mount for support directly under the front where the tractor axels would mount as shown for both the 48-foot trailer and A-Train trailer.	 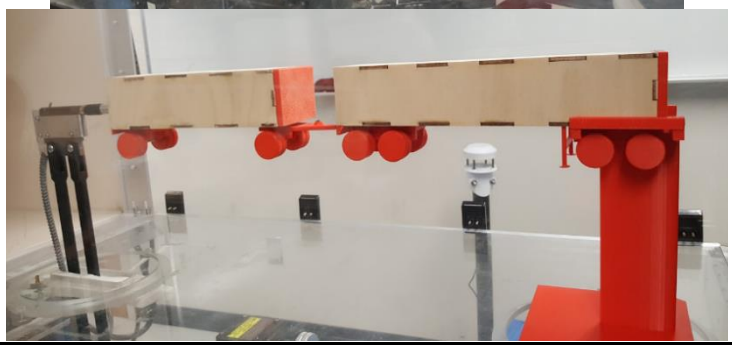
5	Set magnets on the underside of the wind tunnel directly under the airfoil support.	

6	Level the model by adjusting the pitch with the knob shown in top picture. Level the roll of the model by swiveling the model with your hands.	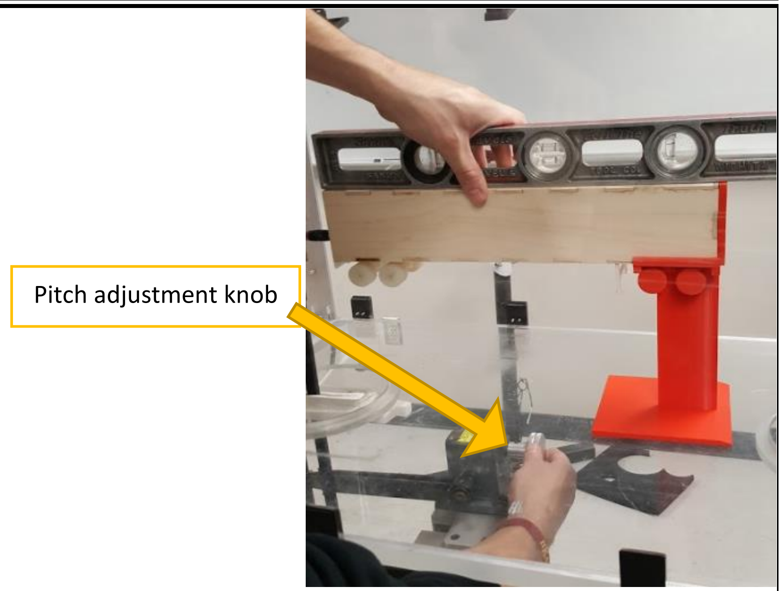 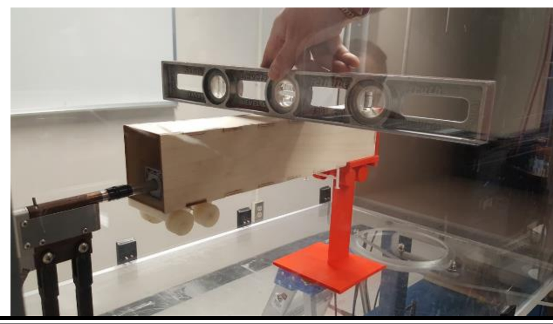
7	Unlock main power breaker and turn to the ON position	

8	Press “Local Remote”. If the display does not read 12.5Hz, click the up arrow until it does. Press “Read Write” to write the displayed frequency to the motor. Press “Run” to turn the fan on. Let the fan run for about 1 minute to achieve the displayed frequency. Use the up and down arrows to adjust speed of the fan. **CAUTION** Ensure lid to the wind tunnel is properly mounted and attached and the safety ropes are installed before running.	

Appendix C

Matlab Scripts

Part 1: Code used for Single Trailer Data Calculations

```
%%% 48' Nose Cone Data Processing
clc
clear
close all

%%% Note - N: No Nose Cone
%%%        C: Nose Cone
%%%        B: Bull Nose

%% Reading Voltage Data from .xlsx files
Frequency = xlsread('Drag Data 48foot Trailer','48-foot Nose Cone','B4:B11');
Display_Force = xlsread('Drag Data 48foot Trailer','48-foot Nose
Cone','E4:E11');
Display_Force_Hopper = xlsread('Drag Data 48foot Trailer','48-foot Nose
Cone','E16:E23');
Display_Force_Possum = xlsread('Drag Data 48foot Trailer','48-foot Nose
Cone','E28:E35');

%% Applying the scaling factor to the drag forces
Scale_Force = (Display_Force - 0.0036)./0.9944;
Scale_Force_Hopper = (Display_Force_Hopper - 0.0036)./0.9944;
Scale_Force_Possum = (Display_Force_Possum - 0.0036)./0.9944;

%% Defining the Relationship between Frequency Drive and Wind Velocity
m_Vel = 1.2081; %(m/s)/Hz
b_Vel = -1.0632; %m/s

for n = 1:length(Frequency)
    V(n,1) = m_Vel*Frequency(n,1) + b_Vel; %m/s
end

V_mph = 2.23694*V;

%% Calculating the Coefficient of Drag on the Trailer
% Constants
rho = 1.225;        %kg/m^3
mu = 1.846e-5;      %kg/m*s
w = 0.0678;         %m (2.671 inches)
h = 0.0762;         %m (3.000 inches)
L = 0.3815;         %m (15.02 inches)
A = w*h;            %m^2

% Calculation
C_Drag = (2*abs(Scale_Force))./(rho*(V.^2)*A);
C_Drag_Hopper = (2*abs(Scale_Force_Hopper))./(rho*(V.^2)*A);
C_Drag_Possum = (2*abs(Scale_Force_Possum))./(rho*(V.^2)*A);
```

```
%% Determining the average Cd for each model
C_Drag_AvgC = mean(C_Drag);
C_Drag_Hopper_AvgC = mean(C_Drag_Hopper);
C_Drag_Possum_AvgC = mean(C_Drag_Possum);

%% Percent Changes in Drag Coefficient w.r.t base model
Hopper_ChangeC = (abs(C_Drag_AvgC - C_Drag_Hopper_AvgC)/C_Drag_AvgC)*100;
Possum_ChangeC = (abs(C_Drag_AvgC - C_Drag_Possum_AvgC)/C_Drag_AvgC)*100;

%% Uncertainty Analysis
U_FD = 0.00454;     %N
U_V = 1;            %m/s
U_rho = 0.0001;     %kg/m^3
U_A = 0.00001;      %m^2
CD_FD = 1/((1/2)*rho*A*V.^2);

%No undercarriage
CD_rho = (-Scale_Force)./((1/2)*rho^2*A*V.^2);
CD_A = (-Scale_Force)./((1/2)*rho*A^2*V.^2);
CD_V = (-2*Scale_Force)./((1/2)*rho*A*V.^3);
U_CD = ((CD_FD*U_FD).^2 + (CD_rho*U_rho).^2 + (CD_A*U_A).^2 +
(CD_V*U_V).^2).^(1/2);

%Hopper Bins
CD_rho_Hopper = (-Scale_Force_Hopper)./((1/2)*rho^2*A*V.^2);
CD_A_Hopper = (-Scale_Force_Hopper)./((1/2)*rho*A^2*V.^2);
CD_V_Hopper = (-2*Scale_Force_Hopper)./((1/2)*rho*A*V.^3);
U_CD_Hopper = ((CD_FD*U_FD).^2 + (CD_rho_Hopper*U_rho).^2 +
(CD_A_Hopper*U_A).^2 + (CD_V_Hopper*U_V).^2).^(1/2);

%Possum Belly
CD_rho_Possum = (-Scale_Force_Possum)./((1/2)*rho^2*A*V.^2);
CD_A_Possum = (-Scale_Force_Possum)./((1/2)*rho*A^2*V.^2);
CD_V_Possum = (-2*Scale_Force_Possum)./((1/2)*rho*A*V.^3);
U_CD_Possum = ((CD_FD*U_FD).^2 + (CD_rho_Possum*U_rho).^2 +
(CD_A_Possum*U_A).^2 + (CD_V_Possum*U_V).^2).^(1/2);

%% Plotting Results
figure(2)
set(gcf,'color','w')
% plot(V_mph,C_Drag,'k.--','Linewidth',2,'MarkerSize',30)
errorbar(V_mph,C_Drag,U_CD(:,1),'k.--','Linewidth',1.5,'MarkerSize',15)
hold on
% plot(V_mph,C_Drag_Hopper,'b.--','Linewidth',2,'MarkerSize',30)
errorbar(V_mph,C_Drag_Hopper,U_CD_Hopper(:,1),'b.--
','Linewidth',1.5,'MarkerSize',15)
% plot(V_mph,C_Drag_Possum,'r.--','Linewidth',2,'MarkerSize',30)
errorbar(V_mph,C_Drag_Possum,U_CD_Possum(:,1),'r.--
','Linewidth',1.5,'MarkerSize',15)
title('C_{D} of a 48'' Trailer with a Nose Cone','Fontname','Times',...
    'Fontweight','bold','Fontsize',16)
xlabel('Velocity [mph]','Fontname','Times','Fontweight','bold','Fontsize',13)
ylabel('C_{D}','Fontname','Times','Fontweight','bold','Fontsize',13)
ylimits = [0 1];
```

```
ylim(ylimits)
legend('Location','southeast',['Base Model - C_{D} =
',num2str(C_Drag_AvgC,2),...
    '; %{\Delta} = N/A'],['Hopper Bins - C_{D} =
',num2str(C_Drag_Hopper_AvgC,2),...
    '; %{\Delta} = ',num2str(Hopper_ChangeC,3)],['Possum Belly - C_{D} =
',...
    num2str(C_Drag_Possum_AvgC,2),'; %{\Delta} =
',num2str(Possum_ChangeC,3)])
grid on
box off

%% Emission Calculations
CD_BaseNNC = 0.7042;
C1 = 117.8;
C2 = 1.78;
C3 = -9.48;
C4 = -0.00258;
C5 = 1.00;          %Tire Inflation System
TRRL = 4.6;         %Tire Rolling Resistance Level
WR = 655;           %Weight Reduction
h_48 = 2.92;        %m
w_48 = 2.49;        %m
A_48 = h_48*w_48;   %m^2

e_CO2_C = (C1 + C2*TRRL + C3*(abs(CD_BaseNNC - C_Drag_AvgC)*A_48)...
    + C4*WR)*C5  %gCO2/ton-mile
e_CO2_HopperC = (C1 + C2*TRRL + C3*(abs(CD_BaseNNC -
C_Drag_Hopper_AvgC)*A_48)...
    + C4*WR)*C5  %gCO2/ton-mile
e_CO2_PossumC = (C1 + C2*TRRL + C3*(abs(CD_BaseNNC -
C_Drag_Possum_AvgC)*A_48)...
    + C4*WR)*C5  %gCO2/ton-mile

FC_C = (e_CO2_C/10180)*1000 %gal_diesel/1000ton-mile
FC_HopperC = (e_CO2_HopperC/10180)*1000 %gal_diesel/1000ton-mile
FC_PossumC = (e_CO2_PossumC/10180)*1000 %gal_diesel/1000ton-mile
```

Part 2: Code used for A-Train Data Calculations

```
%%% A-Train 4.47" length data processing
clc
clear
% close all

%%% Note - N: No Nose Cone
%%%        C: Nose Cone
%%%        B: Bull Nose

%% Reading Data from .xlsx files
Frequency = xlsread('Drag Data A-Train Trailer','A-Train 4.47','B5:B12');
Display_ForceN = xlsread('Drag Data A-Train Trailer','A-Train
4.47','E17:E24');
Display_ForceC = xlsread('Drag Data A-Train Trailer','A-Train
4.47','K17:K24');

%% Applying the scaling factor to the drag forces
Scale_ForceN = (Display_ForceN - 0.0036)./0.9944;
Scale_ForceC = (Display_ForceC - 0.0036)./0.9944;

%% Defining the Relationship between Frequency Drive and Wind Velocity
m_Vel = 1.2081; %(m/s)/Hz
b_Vel = -1.0632; %m/s

for n = 1:length(Frequency)
    V(n,1) = m_Vel*Frequency(n,1) + b_Vel; %m/s
end

V_mph = 2.23694*V;

%% Calculating the Coefficient of Drag on the Trailer
% Constants
rho = 1.225;          %kg/m^3
mu = 1.846e-5;        %kg/m*s
w = 0.0650;           %m (2.560 inches)
h = 0.0518;           %m (2.039 inches)
A = w*h;              %m^2

% Calculation
C_DragN = (2*abs(Scale_ForceN))./(rho*(V.^2)*A);
C_DragC = (2*abs(Scale_ForceC))./(rho*(V.^2)*A);

%% Determining the average Cd for each model
C_Drag_AvgN = mean(C_DragN);
C_Drag_AvgC = mean(C_DragC);

%% Percent Changes in Drag Coefficient w.r.t base model
ChangeC = (abs(C_Drag_AvgN - C_Drag_AvgC)/C_Drag_AvgN)*100;

%% Uncertainty Analysis
U_FD = 0.00454;      %N
```

```
U_V = 1;            %m/s
U_rho = 0.0001;     %kg/m^3
U_A = 0.00001;      %m^2
CD_FD = 1/((1/2)*rho*A*V.^2);

%No Nose Cone
CD_rho_N = (-Scale_ForceN)./((1/2)*rho^2*A*V.^2);
CD_A_N = (-Scale_ForceN)./((1/2)*rho*A^2*V.^2);
CD_V_N = (-2*Scale_ForceN)./((1/2)*rho*A*V.^3);
U_CD_N = ((CD_FD*U_FD).^2 + (CD_rho_N*U_rho).^2 + (CD_A_N*U_A).^2 +
(CD_V_N*U_V).^2).^(1/2);

%Nose Cone
CD_rho_C = (-Scale_ForceC)./((1/2)*rho^2*A*V.^2);
CD_A_C = (-Scale_ForceC)./((1/2)*rho*A^2*V.^2);
CD_V_C = (-2*Scale_ForceC)./((1/2)*rho*A*V.^3);
U_CD_C = ((CD_FD*U_FD).^2 + (CD_rho_C*U_rho).^2 + (CD_A_C*U_A).^2 +
(CD_V_C*U_V).^2).^(1/2);

%% Plotting Results
figure(1)
set(gcf,'color','w')
% plot(V_mph,C_DragN,'k.--','Linewidth',2,'MarkerSize',30)
errorbar(V_mph,C_DragN,U_CD_N(:,1),'k.--','Linewidth',1.5,'MarkerSize',15)
hold on
% plot(V_mph,C_DragC,'b.--','Linewidth',2,'MarkerSize',30)
errorbar(V_mph,C_DragC,U_CD_C(:,1),'b.--','Linewidth',1.5,'MarkerSize',15)
title('C_{D} of A-Train Trailers at 7''-1"','Fontname','Times',...
    'Fontweight','bold','Fontsize',16)
xlabel('Velocity [mph]','Fontname','Times','Fontweight','bold','Fontsize',13)
ylabel('C_{D}','Fontname','Times','Fontweight','bold','Fontsize',13)
ylimits = [0 1.2];
ylim(ylimits)
legend('Location','southeast',['Base Model - C_{D} =
',num2str(C_Drag_AvgN,2),...
    '; %{\Delta} = N/A'],['Nose Cone - C_{D} = ',num2str(C_Drag_AvgC,2),...
    '; %{\Delta} = ',num2str(ChangeC,3)])
grid on
box off

%% Emission Calculations
CD_902NNC = 0.9179;
C1 = 117.8;
C2 = 1.78;
C3 = -9.48;
C4 = -0.00258;
C5 = 1.00;              %Tire Inflation System
TRRL = 4.6;             %Tire Rolling Resistance Level
WR = 655;               %Weight Reduction
h_48 = 1.99;            %m
w_48 = 2.49;            %m
A_ATrain = h_48*w_48;   %m^2

e_CO2_N = (C1 + C2*TRRL + C3*(abs(CD_902NNC - C_Drag_AvgN)*A_ATrain)...
    + C4*WR)*C5  %gCO2/ton-mile
e_CO2_C = (C1 + C2*TRRL + C3*(abs(CD_902NNC - C_Drag_AvgC)*A_ATrain)...
```

```
    + C4*WR)*C5  %gCO2/ton-mile

FC_N = (e_CO2_N/10180)*1000 %gal_diesel/1000ton-mile
FC_C = (e_CO2_C/10180)*1000 %gal_diesel/1000ton-mile
```

Appendix D

Scale Model Drawings

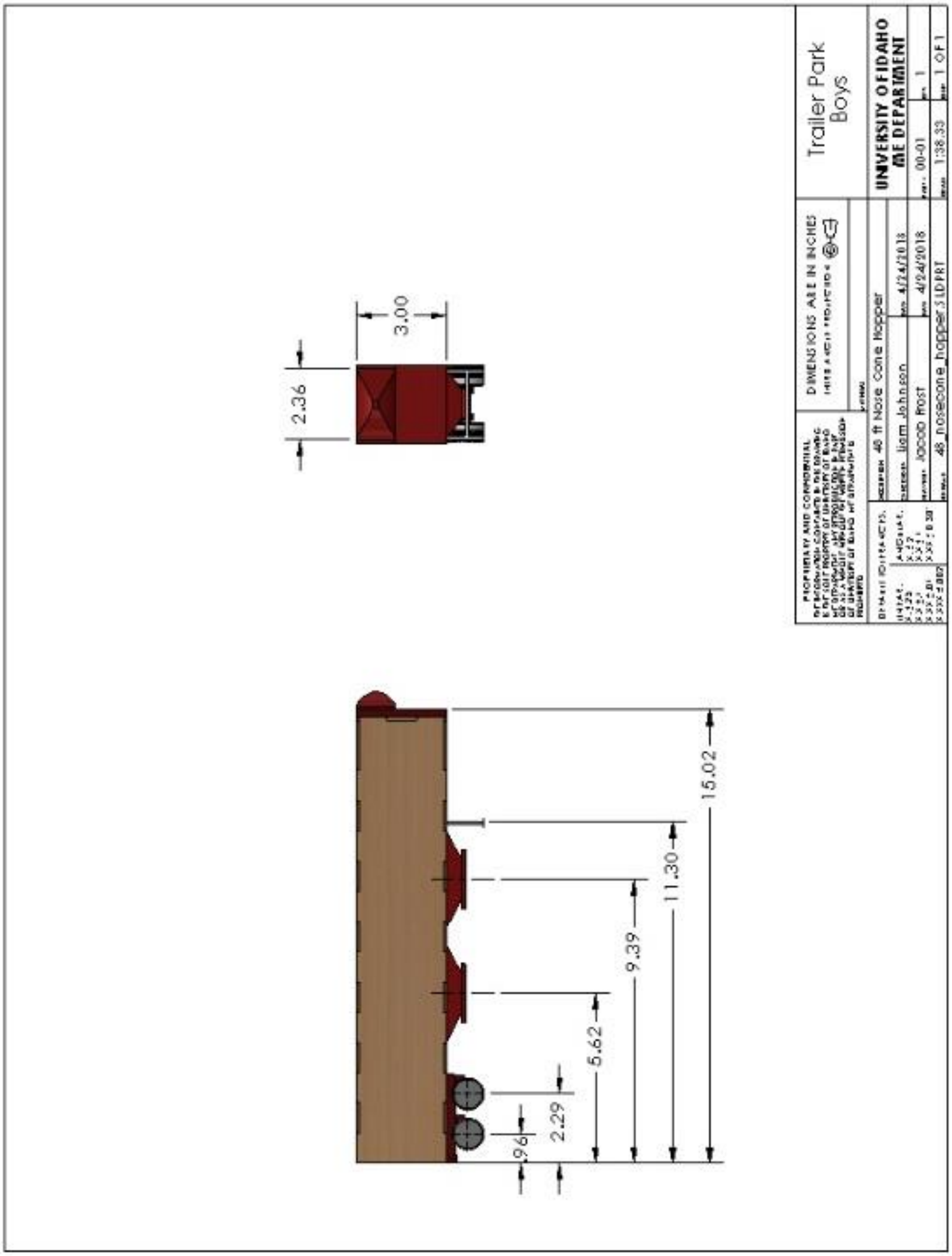

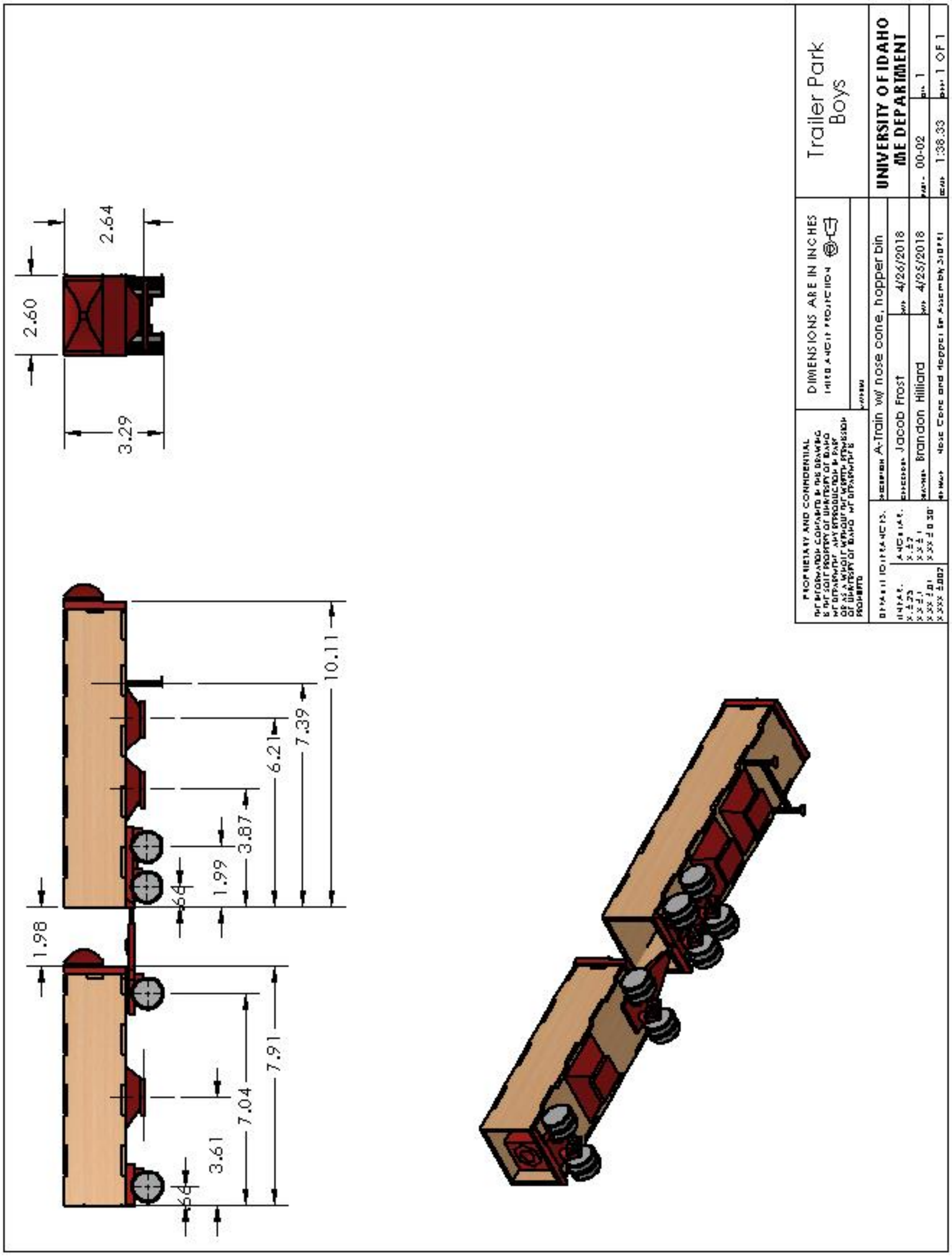

Trailer Park Boys
UNIVERSITY OF IDAHO
ME DEPARTMENT
DIMENSIONS ARE IN INCHES
A-Train w/ nose cone, hopper bin
Jacob Frost
4/26/2018
Brandon Hilliard
4/25/2018
00-02
1
1:38.33
1 OF 1
2.60
2.64
3.29
1.98
10.11
7.39
6.21
3.87
1.99
.64
7.91
7.04
3.61
.64